

2012

Flexural Behavior of Laterally Damaged Full-Scale Bridge Girders Through the Use of Carbon Fiber Reinforced Polymers (CFRP)

Nicholas James Alteri

College of Computing, Construction and Engineering

Suggested Citation

Alteri, Nicholas James, "Flexural Behavior of Laterally Damaged Full-Scale Bridge Girders Through the Use of Carbon Fiber Reinforced Polymers (CFRP)" (2012). *UNF Graduate Theses and Dissertations*. 412.
<https://digitalcommons.unf.edu/etd/412>

This Master's Thesis is brought to you for free and open access by the Student Scholarship at UNF Digital Commons. It has been accepted for inclusion in UNF Graduate Theses and Dissertations by an authorized administrator of UNF Digital Commons. For more information, please contact [Digital Projects](#).

© 2012 All Rights Reserved

**FLEXURAL BEHAVIOR OF LATERALLY DAMAGED FULL-SCALE BRIDGE
GIRDERS THROUGH THE USE OF CARBON FIBER REINFORCED
POLYMERS (CFRP)**

By
Nicholas James Alteri

A thesis submitted to the Department of Engineering
in partial fulfillment of the requirements for the degree of

Master of Science in Civil Engineering

UNIVERSITY OF NORTH FLORIDA

COLLEGE OF ENGINEERING

OCTOBER, 2012

Unpublished work c Nicholas James Alteri

Acknowledgements

The author would like to thank the faculty of the civil engineering department at the University of North Florida for the preparation given to approach a research project of this proportion. Special thanks are given to the members of his research committee Dr. Adel El-Safty (Advisor and Committee Chair), Dr. Mike Jackson and Dr. Thobias Sando for their inspiration and guidance throughout the execution of this research project. Very much appreciation is given to the Florida Department of Transportation (FDOT) for the support that was given and the interest that they had shown throughout the research project. The author thanks the Fyfe Corporation and the BASF corporation for their contributions of the materials used in the research project.

The author would like to give a very special thanks to family Al, Theresa, Tony and Mollie Alteri for their support throughout all of the research. The author shows very much appreciation to his friends for their encouragement from the start to the finish of the research.

Table of Contents

Acknowledgements	iv
Table of Contents	v
Chapter 1 – Introduction	1
1.1 – Background	3
1.2 – Hypothesis	4
1.3 – Objectives	5
Chapter 2 - Literature Review	7
2.1 – Introduction	7
2.2 - Previous Repair Methods	7
2.2.1 Metal Sleeve Splicing	8
2.2.2 Strand Splicing	9
2.2.3 External Post Tensioning	9
2.2.4 Near Surface Mounted (NSM) CFRP	9
2.3 - Material Properties	10
2.3.1 Uniaxial, Biaxial and Tri-axial fibers	10
2.3.2 Fiber Materials and Adhesives	11
2.4 Flexural and Shear Behavior	12
2.4.1 Static Behavior	13
2.4.2 Fatigue Behavior	13
2.4.3 Behavior in Shear	14
2.4.5 Laterally Damaged Bridge Girders	16
2.5 Failure Modes	18
2.5.1 Concrete crushing	18
2.5.2 CFRP Rupture	18
2.5.3 Debonding of CFRP laminates	19
2.5.4 Prestressing Steel Rupture	20
2.5.5 Shear Failure	21
Chapter 3 - Experimental Program	22
3.1 – Materials	22
3.2 – Test Girders	26
3.2.1 Girder Geometry and Cross-Section Properties	26

3.2.2 Steel Reinforcement and Strand Designation	27
3.2.3 Simulated Damage	30
3.3 Test Setup	31
3.4 Instrumentation	33
3.4.1 Stain Gauges	33
3.4.2 LVDT's	34
3.5 Repair Configurations	35
Chapter 4 – Results	39
4.1 Control Girders	39
4.1.1 Control Girder 8 (undamaged Control)	40
4.1.2 Control Girder 4 (Simulated Lateral Damage)	42
4.2 Damaged and Repaired Girders	45
4.2.1 Repaired Girder 5	45
4.2.2 Repaired Girder 6	48
4.2.3 Repaired Girder 7	51
Chapter 5 –Analysis	56
5.1 – Introduction	56
5.2 - Pre-stress Loss Calculations	56
5.3 - Capacity Calculations	59
5.4 – Shear Calculations	65
5.5 - Deflection Calculations	67
5.5.1 - Effective Moment Of Inertia Method	67
5.5.2 - Bilinear Method	69
5.6 – Limitations	73
Chapter 6 - Discussion and Conclusions	75
6.1 – Summary of Findings	75
6.2 – Conclusions	76
References	78
Appendix A – Excel Model Screen Shots	81

ABSTRACT

The repair and strengthening of concrete bridge members with CFRP has become increasingly popular over recent years. However, significant research is still needed in order to develop more robust guidelines and specifications. The research project aims to assist with improving design procedures for damaged concrete members with the use of CFRP.

This document summarizes the analysis and testing of full-scale 40' foot long prestressed concrete (PSC) bridge girders exposed to simulated impact damage and repaired with carbon fiber reinforced polymers (CFRP) materials. A total of five AASHTO type II bridge girders fabricated in the 1960's were taken from an existing bridge, and tested at the Florida Department of Transportation FDOT structures lab in Tallahassee, Florida. The test specimens were tested under static loading to failure under 4-point bending.

Different CFRP configurations were applied to each of the girders. Each of the test girders performed very well as each of them held a higher capacity than the control girder. The repaired girders 5, 6 and 7 surpassed the control girder's capacity by 10.88%, 15.9% and 11.39%. These results indicate that repairing laterally damaged prestressed concrete bridge girders with CFRP is an effective way to restore the girders flexural capacity.

Chapter 1

Introduction

The deterioration of concrete bridge structures around the world is an ongoing issue that must be studied and analyzed for better solutions for the repair and strengthening of these structures. In addition to loss in flexural capacity vehicle collisions often cause the structure to be vulnerable to corrosion damage because they can leave exposed steel reinforcements which is detrimental to the integrity of the structure. A nationwide survey showed that on average, in the United States between twenty-five and thirty-five bridges are damaged every year in each state by colliding over-height vehicles. (Fu et al, 2003). Vehicular collisions can cause concrete spalling, exposed and/or severed reinforcement, yielding of steel, concrete cracking and even complete structural failure. In extreme cases, when an over-height vehicle strikes a bridge, there may be very little time to restore the capacity of the damaged member or structure before the crossing traffic may cause catastrophic failure. Figure 1.1 shows an example of a bridge that was struck by an over-height vehicle which had resulted in the loss of the concrete cross section and severed prestressing strands.



Figure 1.1 – Example of impact damaged bridge girder provided by the Washington State Department of Transportation (WSDOT)

Over the years, there have been many investigations and repair techniques used to combat the problems associated with impact damage from over-height vehicles. Some of the procedures used to repair the damage done to bridge girders from the impact of over-height vehicles can be costly, time consuming and possibly even ineffective. Using Carbon Fiber Reinforced Polymers (CFRP) to repair bridge girders that are damaged by over-height vehicles has become a more acceptable repair method in recent years. The use of CFRP composites offers a quick and economical way to repair and even strengthen damaged bridges.

This research was conducted to demonstrate the effective use of CFRP sheets applied using a wet layup procedure with an epoxy adhesive, in repairing full scale bridge girders with simulated impact damage. The objective of this study was to identify the optimum design configuration for CFRP placement. The variables to be considered included the number of layers on the girder soffit, U-wrap spacing and longitudinal layers placed on the sides of the bottom flange, web and over the top section of U-wraps.

Increasing the number of layers on the girder soffit increases the flexural capacity of the girder while the U-wrappings help to mitigate debonding failures and increase in shear capacity. Figure 1.2 shows the typical wrapping schemes for CFRP sheets.

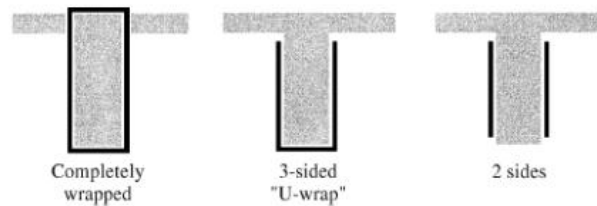


Figure 1.2 - Typical wrapping schemes for strengthening in shear with CFRP sheets provided by ACI 440.2R-08

The longitudinal strips along the bottom flange and web help to mitigate crack propagations from the damaged area. The top strip over the top of the U-wraps was intended to keep U-wraps from debonding.

1.1 Background

Many attempts have been made to identify an efficient way of repairing bridge girders damaged by over-height vehicles. These include external post-tensioning, steel jacketing, strand splicing, or just replacing the girder itself. Research into the use of CFRP sheets to strengthen undamaged concrete members has shown increases in capacities of up to 200% (Grace et al, 1999). Using CFRP sheets offers many advantageous characteristics compared to other methods that are used in the field today. CFRP is very lightweight with a very high ultimate strength, cost effective, quick to install, very resistant to corrosion, and does not alter the shape of the member maintaining the original height of the structure. However, limited design specifications using CFRP sheets for this type of repair have hindered more widespread use. Although federal, state, and local codes for the design of externally bonded CFRP systems do not

exist, other applicable code requirements may influence the selection, design, and installation of the CFRP system (ACI Committee 440, 2008).

The ACI 440.2R-08 document contains guidelines for different applications of CFRP sheets on different concrete structural members, yet topics such as debonding and durability need to be further researched. “For long span FRP plated reinforced concrete, with the longitudinal strengthening extending to near the supports, the common failure mode is interface debonding propagating from flexural cracks around midspan towards the supports” (Rosenboom and Rizkalla 2006). “However, based on the available research, the design procedures outlined in this document are considered to be conservative” (ACI Committee 440, 2008).

Along with debonding and durability, some other areas where there is a lack of research include fatigue behavior, deflection calculations of prestressed members, and the repair of laterally damaged members. There is plenty of research that shows that CFRP sheets can strengthen concrete members and even repair cracked members due to increases in loading, but research on the repair of laterally and severely damaged structures is limited. “There have been several impact-damaged prestressed concrete girders repaired in the field, but a limited number of studies have been conducted in a laboratory setting” (Miller, Rosenboom and Rizkalla 2006).

1.2 Hypothesis

The testing documented herein involves the repair of laterally damaged full-scale AASHTO type II bridge girders through the use of CFRP sheets. Figure 1.3 shows the cross section properties of an AASHTO type II girder.

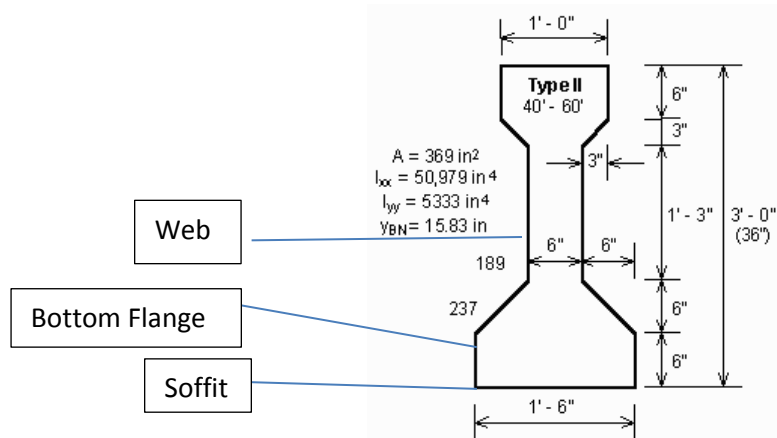


Figure 1.3 – Typical cross section of AASHTO type II girder

The overall objective of the experiment was to provide data to prove laterally damaged bridge girders can be repaired to full capacity and beyond through the use of CFRP sheets. Different methods were explored to help mitigate problems such as debonding and crack propagation in areas of concern to help increase the overall performance of the repair.

Five full-scale 40 feet long prestressed concrete bridge girders with simulated lateral damage were tested under static loading conditions. Based on the results of these experiments, it is believed that recommendations for CFRP sheet configurations and calculations can be provided for safer and more efficient repair methods. Observations of the U-wrap configurations were also made to reduce, understand, and predict the debonding failures associated with their spacing that will help to create better configurations of concrete members repaired with CFRP sheets.

1.3 Objectives

This study provides contributions to the study of flexural performance of laterally damaged prestressed bridge girders repaired with CFRP. The CFRP sheets applied to the girder soffit in the longitudinal direction provide flexural strengthening, which increases

with the number of layers. The U-wrap configurations are used as anchorages to help reduce debonding failures as well as increase shear capacity. The longitudinal strips on the bottom flange and the web of each girder are to help mitigate crack propagations. These parameters were closely observed during testing to identify the optimum configuration for the repair of the girders with CFRP. A spreadsheet model was also created to calculate the girder capacities and deflections of both reinforced concrete and prestressed concrete girders repaired and strengthened with CFRP sheets for design and analysis purposes. The bilinear method and the effective moment of inertia method were used to calculate the deflections of each of the girders.

Chapter 2

Literature Review

2.1 Introduction

Through the review of literature, this chapter provides an introduction to the repair and strengthening of reinforced and prestressed concrete bridge girders through the use of CFRP. Special consideration is taken into account with the investigations of the behavior of these members under static loading, fatigue/cyclic loading, strengthening in shear and failure modes. There is also consideration in the different types of CFRP sheets, adhesives, and configurations.

2.2 Previous Repair Methods

Over the years, there have been many different methods created to repair damaged bridge girders, but most of them are time consuming, expensive or maybe not even effective. These repairs include strand splicing, metal sleeve splicing/steel jacketing, and external post tensioning. NCHRP Report 226 by Shanafelt and Horn in 1980 goes into significant detail into the repair of impact damaged bridge girders with different methods and suggested repair techniques based on the level of damage. NCHRP report 226 gives three different levels of damage severity which are as follows:

***MINOR:** damage is defined as concrete with shallow spalls, nicks and cracks, scrapes and some efflorescence, rust or water stains. Damage at this level does not affect member capacity. Repairs are for aesthetic or preventative purposes.*

***MODERATE:** damage includes larger cracks and sufficient spalling or loss of concrete to expose strands. Moderate damage does not affect member capacity. Repairs are intended to prevent further deterioration.*

***SEVERE:** damage is any damage requiring structural repairs. Typical damage at this level includes significant cracking and spalling, corrosion and exposed and broken strands.*

The choice of repair technique for an impact damaged bridge girder is dictated by the level of damage done to the girder. If the damage is too severe, the member will not be able to be repaired and will need to be replaced. In 2009, Kasan and Harries subdivided the severe category into three different cases. The first case is determined by whether the girder could be repaired without restoring prestressing lost to the damage. The second case says that prestressing needs to be restored. The third case says that the member is too damaged and needs to be replaced.

2.2.1 Metal Sleeve Splicing

Metal Sleeve Splicing is a process where steel plates are used to encase the damaged structural member. This process can be very time consuming and expensive and it also changes the geometry of the specimen. This repair method has been shown to be effective in the repair of large numbers of damaged strands. “When splicing 6 strands or less, the sleeve should lap the severed strands a minimum of 5 feet- 3 inches (1.60 meters), and for splicing more than 6 strands, the sleeve should lap the severed strands 160 strand diameters”(Feldman et al, 1994).

2.2.2 Strand Splicing

Strand splicing is a method used to reconnect a severed prestressing strand and apply post tensioning to it after it is reconnected. The use of strand splicing is effective, but can be problematic due to the geometry of the girder, amount of concrete cover and spacing of different strands. Harries, Kasan and Aktas did research on the use of strand splicing to repair damaged bridge girders, and found that using this method was capable of restoring the capacity and even strengthening the damaged bridge girders (Harries et al, 2009). Zobel and Jirsa also tested different types of strand splicing and found that it had a very high sensitivity to fatigue loading conditions (Zobel and Jirsa, 1998).

2.2.3 External Post Tensioning

The method of external post tensioning involves bonding brackets to the side of the concrete member with prestressing strands placed in the brackets. These strands, steel rods or bars are generally placed on the sides of the girder, but are sometimes placed on the bottom of the girder as well. Once in place, the strands are tensioned by jacking against the brackets to restore the prestressing that was lost with the damage. The size and strength of the jacking corbels also dictate the number of severed strands that can be repaired by means of external post-tensioning (Feldman et al, 1994).

2.2.4 Near Surface Mounted (NSM) CFRP

Near surface mounted CFRP reinforcing bars are basically rods which are made out of carbon fibers that are similar to steel rebar. NSM bars are mounted in a cut out groove on the surface of the soffit of the girder in the longitudinal direction. This has proven effective in increasing the capacity of damaged girders. There are design

guidelines for strengthening concrete members with NSM bars in the ACI 440.2R document.

NSM CFRP rebar can be prestressed or non-prestressed and have been noted to transfer more stresses to the concrete because they are completely covered in epoxy or other adhesive which gives a better bond to the concrete substrate. Studies have shown that both prestressed and non-prestressed NSM CFRP repairs have shown success to the rehabilitation of the girders ultimate capacity (Nordin et al, 2006 and Casadei et al, 2006).

2.3 Material Properties

CFRP sheets are a combination of fibers and an epoxy matrix. “The overall strength of this composite is equal to the sum of the fiber strength and the strength of the epoxy matrix (Vasiliev and Morozov 2007).” This being said, different epoxies combined with different fibers will yield different moduli of elasticity, which is directly related to the materials ultimate tensile strength.

2.3.1 Uniaxial, Biaxial and Triaxial Braided Fibers

Through the studies of mechanics of materials, it has been observed that the strength of a thin wire is generally higher than the strength of a bulk section of that same material (Vasiliev and Morozov, 2007). This observation is the basis of how a ply of CFRP material is so strong in tension. CFRP sheets are made up of an abundance of long, thin fibers running in the same direction, or even multiple directions woven together to make a sheet. A uniaxial ply is one in which the fibers are running in only one direction, thus giving the ply a high tensile strength in the direction of the fibers. This is desirable if the ply is used to resist a tensile load in the direction of the fibers such as flexural

strengthening on the soffit of the girder. Grace et al. 1999, showed that unidirectional fibers oriented in the vertical direction in addition to longitudinal layers on the soffit can increase capacity, reduce deflections, and reduce risk of rupture. Both Green et al, 2004 and Grace et al, 1999 demonstrated that the girders strengthened with unidirectional fibers held the highest ultimate capacity.

Biaxial plies usually have the fibers oriented perpendicular to each other at 0 and 90 degrees so that they can resist loads in two directions. The fibers with the 0 degree orientation are used for flexural strengthening and the 90 degree fibers work as shear reinforcement. The fibers of a triaxial braid are oriented in three directions, 0, 45 and -45 degrees from each other. An experiment done by Grace et al. in 2003 introduced a new tri-axial braided CFRP to strengthen concrete girders in flexure as well as shear.

2.3.2 Fiber Materials and Adhesives

There are several types of fibers used in the fabrication of CFRP sheets, including glass fibers, aramid fibers, carbon fibers, and boron fibers. Each of these fibers has a different ultimate strength and modulus of elasticity. Along with the type of fiber, the type of adhesive plays an important role in the performance of the strengthened or repaired girder. Different types of adhesives have shown to hold a better bond with the concrete surface which in turn can reduce debonding failures associated with these repairs. The most common adhesives used in fiber repairs are epoxy, polyurethane, vinyl ester and phenolic resins. A study done in 2001 by Lamanna, Bank and Scott, used powder activated fasteners to anchor the CFRP material to the concrete test girders which did not achieve as high of an ultimate strength as the adhesive bonded fibers, but the subjects experienced a much more ductile failure.

Green et al, 2004, from the University of Florida tested impact damaged bridge girders with different types of CFRP sheets and found the best combination to be a CFRP and epoxy resin. Grace et al, 1999 tested strengthened reinforced concrete girders with five different systems and found the combination of glass fibers (GFRP) and an epoxy resin adhesive to give the best results for strengthening flexural concrete members.

There have been other investigations regarding the application of prestressed CFRP sheets as well as flexible adhesives. Wight, Green and Erki investigated the use of prestressed CFRP sheets to strengthen concrete girders in 2001 with very promising results. The tests had shown that all of the girders in the experiment repaired with prestressed CFRP sheets had greater loads at cracking, steel yielding and at ultimate failure along with smaller deflections at midspan. Dai et al, 2005, evaluated the performance of reinforced concrete girders strengthened with CFRP and bonded with a flexible adhesive. This research showed that flexible adhesives used to bond CFRP sheets to strengthen girders held higher ultimate capacities than more brittle adhesives. “However, this technique is favored for the ultimate limit state strengthening purpose only since it contributes less stiffness enhancement under the serviceability limit state” (Dai et al, 2005).

2.4 Flexural and Shear Behavior of Repaired and Strengthened Girders

There have been many studies over the years involving flexural tests of concrete girders repaired with CFRP sheets, yet there is still very much to be learned. The main contributing factor to the strengthening of concrete girders with CFRP sheets is the width and number of layers applied to the girders soffit. When a girder is repaired or strengthened with CFRP, it tends to lose its ductility which in turn causes more brittle

failures. Many research projects tested the performance of the repaired girders through static testing, but there is limited research on the fatigue behavior of repaired girders.

2.4.1 Static Behavior

There is a lot of research offered for the behavior of concrete members strengthened and repaired with CFRP and tested statically with a lot of very favorable results. Static loading is when a girder is tested to failure to obtain its ultimate strength and deflection behavior. The most common loading schemes for static loading is in either three or four point bending. Almost every study involving the repair or strengthening of concrete members with CFRP sheets tests the specimens statically to determine the ultimate strength that the specimens reach after the CFRP sheets are applied.

Most studies that involve concrete strengthening or repair using CFRP are done on reinforced concrete members and have shown to be very successful, but still leaves a lot of room for prestressed members to be researched. “The experimental results indicate that a considerable increase in flexural strength can be achieved if proper measures are taken to prevent debonding of the composite materials from the surface of the concrete (Brena, Wood and Kreger 2003).”

2.4.2 Fatigue Behavior

Fatigue is the damage done to a material through the processes of loading and unloading, which is always happening for bridge girders due to cars and trucks driving over them. Investigations on the behavior of prestressed bridge girders have not been extensively explored, yet there are some significant studies that have been done. This is especially important for prestressed members when the strand stresses are increased, the strands can undergo strand fatigue. Another problem with fatigue is that the girders can

lose a lot of their stiffness during fatigue loading cycles. Due to the fact that most applications of CFRP are to strengthen girders to support increased levels of loading, the investigation of fatigue behavior of strengthened girders is very important.

Despite the lack of research, there have been some very favorable results of experiments done involving the fatigue behavior of girders strengthened with CFRP sheets. When strengthening girders with CFRP, fatigue stress range requirements must be taken into account. In an Experiment done by Larson, Peterman and Rasheed in 2005, five pre-cracked specimens were repaired with CFRP and tested in fatigue and showed that the stress range fatigue requirements can be controlled while still attaining high strength levels. In 2006, Miller, Rosenboom and Rizkalla tested an impact damaged girder strengthened with CFRP in fatigue for the North Carolina Department of Transportation and observed that the test girder withstood over 2 million cycles with little deflections or damage to the repaired area. The girder had been loaded to failure following the fatigue test which had failed outside of the repaired area showing that CFRP repaired section outperformed the undamaged section. Kansas State University did a study in 2005 for the repair of cracked prestressed bridge girders tested in fatigue in 2005 where they were tested under high stress ranges in the prestressing strands which caused the early failure of both specimens.

2.4.3 Behavior in Shear

A lot of times when a girder is strengthened or repaired in flexure, it will be able to sustain a higher load, but it will also lose some of its ductility and can have more brittle failures such as shear failures. This is very important because the girder will be more likely to have shear failure if there is nothing done to compensate for this. There are

a couple ways to increase the shear capacity of a girder through the use of CFRP sheets. These methods include U-Wrapping, or a two sided wrap on the sides of the girder with the fibers pointed in the vertical direction. There is also some help in shear through the use of multidirectional fiber CFRP sheets on the soffit which are either bi-axial or tri-axial.

Document ACI 440.2R-08 contains guidelines and design specifications to strengthen concrete members in shear. This document gives recommendations for shear strengthening based upon the effective strain in CFRP laminates, wrapping scheme (Fully wrapped, bonded u-wraps or bonded face plies), fiber orientation, spacing of the traverse CFRP U-wraps and strips along with reinforcement limits.

In 1997, Hutchinson, Abdelrahman and Rizkalla investigated the use of CFRP sheets to strengthen bridge girders in shear. In the experiment, seven small scale AASHTO girders were strengthened using CFRP to come with the most efficient configuration of the laminates. The experiment also investigated different bonding methods and characteristics for the optimum bond strength between the laminates and the concrete. It was concluded that using CFRP laminates to strengthen a bridge girder's shear capacity was an efficient method. The experiment demonstrated that using diagonal sheets at 45 degrees provides the best reduction in tensile force on the stirrups, but they are more susceptible to debonding due to the shape of AASHTO I-girders.

The strengthening of concrete members in shear without any internal stirrups was done by Razaqpur and Isgor in 2006, which evaluated and compared a few different methods and recommendations for the shear design of concrete members with a new proposed shear method. The methods which were investigated were the ACI committee

440 report, the Canadian Standard CSA S806-02, Japan Society of Civil Engineers (JSCE) shear design method, and Frosch and Tureyen's proposed shear method. The conclusions of the experiment show that the proposed method for shear design by Frosch and Tureyen gave the most closely related predictions with the experimental results than any of the other methods.

2.4.2 Laterally or Impact Damaged Bridge Girders

Every year, there are many bridges struck by over-height vehicles that cause lateral damage to the bridge girder. Vehicular collisions can cause concrete spalling, exposed and/or severed reinforcement, yielding of steel, concrete cracking and even complete structural failure. The research on the repair of impact damaged bridge girders using CFRP laminates is rather limited when studied in the laboratory setting.

A report done by the Alabama DOT and the Auburn University Highway Research Center (AUHRC) for the repair of cracked prestressed concrete girders on i-565, Huntsville, Alabama was done which repaired a bridge that was impacted by an over-height truck and was repaired with CFRP material. The girders were first repaired with mortar to regain the cross sectional properties, then it was repaired with a configuration using design recommendations from the ACI 440.2R-08 document. The testing consisted of a controlled truck loading as well as different thermal conditions. Conclusions of the experiment show that repairing damaged bridge girders with CFRP could handle the controlled truck load without any further crack propagation along with different thermal conditions and has maintained these properties for over two years in the report.

In 2004, Green, Boyd, and Lammert conducted research on the behavior of laterally damaged bridge girders repaired with CFRP sheets. In this experiment, there were a total of six 44 foot long AASHTO type II girders with simulated damage which included a control specimen that was not damaged. The specimens were damaged by removing a 5 foot long section of concrete from the bottom flange on each side at midspan and 4 severed strands on each side of the bottom flange as well which represented about an 18% loss in ultimate strength. The damaged girders were repaired with different types of CFRP sheets and adhesives and found that the girder number 6 which was repaired with CFRP with an epoxy adhesive performed the best. Girder 6 was configured with 3 20x18 inch strips in the longitudinal direction of the soffit and two layers of CFRP U-wraps that covered just up over the bottom flange for anchorages.

In 2004, T. J. Wipf et al, tested the repair of impact damaged bridge girders with CFRP for the Iowa Department of Transportation. They used CFRP material to repair simulated impact damaged bridge girders. The results had shown that the CFRP sheets had restored the flexural strength and increased the cracking load for the test specimens. “As a result of its successful application in the laboratory, CFRP was used to repair three existing prestressed concrete bridges. Although these bridges are still being monitored, results to date indicate the effectiveness of the CFRP (T. J. Wipf et al, 2004).” Another report by Rosenboom, Rizkalla and Miller in 2011 was performed on the repair of five full scale bridge girders and found that the strength, displacement and overall capacity of damaged bridge girders could be restored through the use of CFRP laminates as long as there was the proper application of the CFRP configuration.

2.5 Failure Modes

Reinforced concrete and prestressed concrete girders already experience three different failure modes that include concrete crushing, shear failure, and tension failure. Using CFRP sheets to repair and strengthen concrete members creates additional failure modes to those already associated with concrete girders. The additional failure modes that are encountered are CFRP rupture and the debonding of CFRP sheets from the surface of the concrete. CFRP rupture and debonding are both a very brittle type of failure mode which are usually very quick and unforeseen and can be very catastrophic when encountered in the field.

2.5.1 Concrete Crushing

Concrete crushing is a type of failure that happens when the concrete in the compression zone reaches a compressive strain greater than its maximum which is usually 0.003 in/in. This type of failure can be desirable when CFRP laminates are used to strengthen or repair a concrete member because it shows that the strengthening or repair system has reached the ultimate girder strength and possibly even higher. Many tests result in this type of failure because the girders have been strengthened beyond the limitation that the concrete in compression provides.

2.5.2 CFRP Rupture

Rupture of the CFRP happens when the tensile strain in the CFRP material becomes greater than its ultimate rupture strain. Rupture of the CFRP sheets is sometimes a desirable failure mode when doing experimental research tests in the lab because it will generally occur under ultimate strength conditions, which is considered a mature failure since it reaches the full CFRP tensile strain. Although this failure mode is desirable in the

lab, rupture of the CFRP is a sudden brittle type of failure that should be avoided in the field at all costs. Stress and strain limitations are given by ACI 440 code to account for rupture of the CFRP sheets.

There have been many experiments performed where the rupture of the CFRP material was the main failure mode observed. In 2004, Green et al, experienced a failure due to CFRP rupture on a test girder using one longitudinal E-Glass multidirectional fiber layer and a vinyl ester adhesive on the soffit with a 0.5 inches thick by 24 inches wide sprayed GFRP U-wrapping up to the bottom flange.

2.5.3 Debonding of CFRP Laminates

The ripping or peeling of CFRP sheets from the concrete substrate known as debonding failures which happen when the ultimate debonding strain is achieved and there is cracking between the concrete and CFRP sheets. “While most of the debonding modes have been identified by researchers, more accurate methods of predicting debonding are still needed (ACI Committee 440, 2008).” The code also provides limitations to account for debonding failures for the stress and strain levels achieved in the CFRP.

Sami Rizkalla and Owen Rosenboom did an experiment in 2006 evaluating the bond behavior of CFRP strengthened prestressed bridge girders. Six girders were tested in the experiment configured with either pre-cured CFRP strips or wet layup sheets, U-wraps along the whole girder span or only half, a girder strengthened with pre-cured CFRP strips and debonding mitigation and a control girder which was not strengthened. The test specimens were loaded beyond cracking load, then reloaded to failure to observe the behavior of the crack re-openings. The test girder with U-Wrappings across the whole

length of the girder achieved 72% of the ultimate design strength before the girder failed due to CFRP debonding while the other girders with U-wraps on only one side of the girder tested slightly lower due to premature debonding which was expected for observation purposes. All of the girders strengthened with CFRP in the experiment failed due to intermediate crack debonding except one that failed due to CFRP rupture and one that failed due to intermediate crack debonding followed by rupture of CFRP. “The only girder with debonding mitigation showed considerably more deflection than the others” (Rosenboom & Rizkalla 2007).

Many other experiments researching the strengthening of concrete bridge girders with CFRP sheets have reported failure due to debonding of the CFRP laminates which is usually followed by failure due to CFRP rupture. The debonding has shown to start its occurrence at cracking near the mid-span and work its way toward the ends of the girders. “It was found that sandblasting the concrete surface was only slightly more effective than grinding in controlling debonding” (Wipf et al, 2004). Dai et al, 2005 proposed the repair of damaged girders with CFRP composites using a flexible bond adhesive which showed that the softer adhesives with lower rupture strengths, but high rupture strains can delay the debonding of the interface and increase the ultimate strength. Using flexible adhesives showed that using one and two layers on the soffit was more effective than three, and the spacing of the U-wrap anchorages could also be a factor in lower ultimate strengths.

2.5.4 Prestressing Steel Rupture

The rupturing of prestressing strands occurs when the tensile strain in the strands becomes larger than the ultimate strain. This failure mode is not the most common

amongst concrete members which are repaired or strengthened with CFRP sheets, though it does sometimes occur. Most prestressed girders are designed with prestressing strands made from 270 ksi ultimate strength steel which has a rupture strain of 0.05 in/in. The rupture of prestressing strands in strengthened or repaired concrete members is usually followed by the rupture of the CFRP material as well.

2.5.5 – Shear Failures

When concrete members are strengthened using CFRP laminates, the original shear reinforcement is not adequate enough to handle higher levels of loading. There have been many studies to investigate and improve the shear performance of strengthened and repaired girders through the use of different fabrics and U-wrapping configurations. U-wrapping schemes have proven to be effective to increase the shear capacity as well as mitigate crack propagation due to shear forces of strengthened girders, but shear failures still occur in strengthened girders.

Shear failures were examined by Oral Buyukozturk and Brian Hearing in 1998 when they tested girders retrofitted with CFRP and concluded that the longitudinal strips on the girder soffit did not add any significant strength to the shear capacity of the girders. Other studies such as Grace et al, 1999 and Hutchinson et al, 1997 have shown that different U-wrapping configurations and fibers placed in the traverse direction can significantly increase the shear capacity to reduce this type of failure.

Chapter 3

Experimental Program

3.1 Materials

There are different materials used when repairing an impact damaged bridge girder. The properties of these materials are usually provided by the manufacturer of that specific material. Some of the materials considered are the type of CFRP material, adhesives, concrete, mild and prestressing steel. The type of CFRP material used in the experiment was a uniaxial fiber Fyfe-Tyfo® SCH-41. One of the test specimens was reinforced with Fyfe-Tyfo® SCH-41 material on the soffit while a few of the U-wrappings were done using another uniaxial CFRP that was made by BASF Chemical Company because there was a shortage of the Fyfe material. This was noted, but since the U-wrappings were there as anchorage for the main flexural reinforcement only along with the similar material properties, it was decided that it was fine to use the material. Figure 3.1 shows a picture of the Fyfe material that was used in this study and table 3.1 summarizes the properties of the fiber.

Tyfo® SCH-41 System

Image Redacted.
Available for
viewing at
originating
institution.

Figure 3.1 – Picture of the Fyfe uniaxial CFRP material courtesy of Fyfe.Co.LLC

TYPICAL DRY FIBER PROPERTIES	
PROPERTY	TYPICAL TEST VALUE
Tensile Strength	550,000 psi (3.79 GPa)
Tensile Modulus	33.4 x 10 ⁶ psi (230 GPa)
Ultimate Elongation	1.7%
Density	0.063 lbs./in. ³ (1.74 g/cm ³)
Minimum weight per sq. yd.	19 oz. (644 g/m ²)

Table 3.1 – Dry fiber properties courtesy of Fyfe.Co.LLC

An epoxy adhesive was used to bond the fibers to the concrete surface. The Fyfe-Tyfo® SCH-41 CFRP material was used with a Tyfo® S Saturate which is an epoxy adhesive designed by the manufacturer for that specific type of CFRP. This adhesive was mixed with silica fume to increase the viscosity for better control and placement of the epoxy. Table 3.2 shows the material properties of the cured epoxy.

EPOXY MATERIAL PROPERTIES		
Curing Schedule 72 hours post cure at 140° F (60° C).		
PROPERTY	ASTM METHOD	TYPICAL TEST VALUE*
Tensile Strength ¹	D638 Type 1	10,500 psi (72.4 MPa)
Tensile Modulus	D638 Type 1	461,000 psi (3.18 GPa)
Elongation Percent	D638 Type 1	5.0%
Flexural Strength	D790	17,900 psi (123.4 MPa)
Flexural Modulus	D790	452,000 psi (3.12 GPa)
T _g	D4065	180° F (82° C)

¹ Testing temperature: 70° F (21° C) Crosshead speed: 0.5 in. (13mm)/min. Grips Instron 2716-0055 - 30 kips
* Specification values can be provided upon request.

Table 3.2 – Properties of cured epoxy courtesy of Fyfe.Co.LLC

When the two materials are combined together and allowed to properly cure, the final product has some different properties. Table 3.3 shows the composite gross laminate properties of the materials.

COMPOSITE GROSS LAMINATE PROPERTIES			
PROPERTY	ASTM METHOD	TYPICAL TEST VALUE	DESIGN VALUE*
Ultimate Tensile Strength in Primary Fiber Direction	D3039	143,000 psi (986 MPa) (5.7 kip/in. width)	121,000 psi (834 MPa) (4.8 kip/in. width)
Elongation at Break	D3039	1.0%	0.85%
Tensile Modulus	D3039	13.9 x 10 ⁶ psi (95.8 GPa)	11.9 x 10 ⁶ psi (82 GPa)
Flexural Strength	D790	17,900 psi (123.4 MPa)	15,200 psi (104.8 MPa)
Flexural Modulus	D790	452,000 psi (3.12 GPa)	384,200 psi (2.65 GPa)
Longitudinal Compressive Strength	D3410	50,000 psi (344.8 MPa)	42,500 psi (293 MPa)
Longitudinal Compressive Modulus	D3410	11.2 x 10 ⁶ psi (77.2 GPa)	9.5 x 10 ⁶ psi (65.5 GPa)
Longitudinal Coefficient of Thermal Expansion	D696	3.6 ppm./°F	
Transverse Coefficient of Thermal Expansion	D696	20.3 ppm./°F	
Nominal Laminate Thickness		0.04 in. (1.0mm)	0.04 in. (1.0mm)

Table 3.3 – Composite gross laminate properties courtesy of Fyfe.Co.LLC

The CFRP material used for the U-wraps of girder 6 was a little different than the Fyfe-Tyfo® SCH-41 used for the other girders. The material used was called MBrace®

CF 160 provided by the BASF Chemical Company. The properties of this carbon fiber material can be seen in figures 3.4 and 3.5 below.

Physical Properties		0° Tensile Properties ^(2,3)	
PROPERTY	VALUE	PROPERTY	VALUE
Fiber Material	High Strength Carbon	Ultimate Tensile Strength, f_{tu}^*	550 ksi [3800 MPa]
Fiber Tensile Strength [MPa]	720 ksi [4950]	Tensile Modulus, E_f	33000 ksi [227 GPa]
Areal Weight	0.124 lb/ft ² [600 g/m ²]	Ultimate Tensile Strength per Unit Width, $f_{tu}^* t_f$	7.14 kips/in/ply [1.25 kN/mm/ply]
Fabric Width	20 in 500 mm	Tensile Modulus per Unit Width, $E_f t_f$	430 kips/in/ply [76 kN/mm/ply]
Nominal Thickness, T_f^m	0.013 in/ply [0.33 mm/ply]	Ultimate Rupture Strain, ϵ_{fu}^*	1.67%

Table 3.4 - Physical and tensile properties of the MBrace® CF 160 provided by BASF the Chemical Company

The MBrace® CF 160 material used a different epoxy adhesive saturant than the Fyfe-Tyfo® SCH-41 as well. The saturant that was used to bond the MBrace® CF 160 CFRP to the concrete substrate was MBrace® Saturant LTC which was a two part blue mixture. The tensile and flexural properties of the MBrace® Saturant LTC can be seen in Table 3.5 below.

Tensile Properties (1)		Flexural Properties (3)	
PROPERTY	VALUE	PROPERTY	VALUE
Yield Strength	2100 psi (14 MPa)	Yield Strength	3600 psi (25 MPa)
Strain at Yield	1.3%	Strain at Yield	4.5%
Elastic Modulus	165 ksi (1138 MPa)	Elastic Modulus	80 ksi (552 MPa)
Ultimate Strength	2100 psi (14 MPa)	Ultimate Strength	3600 psi (25 MPa)
Rupture Strain	5.3%	Rupture Strain	5%
Poisson's Ratio	0.40		

Table 3.5 – Tensile and flexural properties of the MBrace® Saturant LTC provided by BASF the Chemical Company

From the stress strain diagram in figure 3.2 below shows CFRP in tension which is linear up until failure showing how brittle of a material CFRP is.

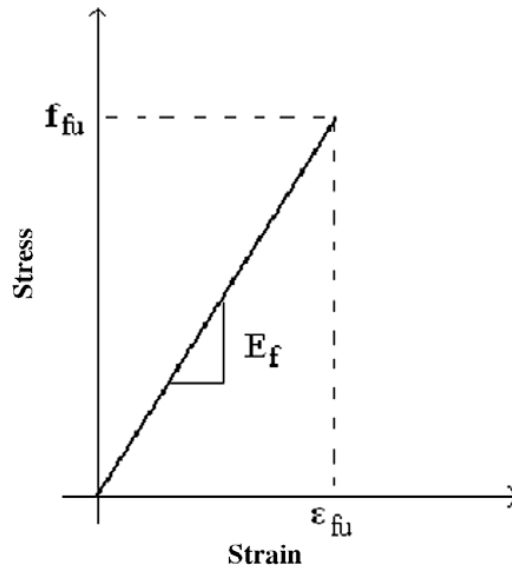


Figure 3.2 - Stress/Strain curve for CFRP in tension provided by Akbarzadeh and Maghsoudi 2009

3.2 Test Girders

The research presented in this experiment investigates the flexural behavior of five full-scale 40 feet long prestressed concrete girders that have simulated lateral damage repaired with CFRP sheets. The bridge girders used in the experiment were taken from an existing bridge in Florida. They were fabricated in the 1960's and held at the Florida Department of Transportation (FDOT) where the experiment took place. These five girders were tested under static loading conditions including two control girders, one of which was undamaged and another with simulated lateral damage induced to it without any repair.

3.2.1 Girder Geometry

Each of the test specimens was a prestressed AASHTO type II girder that had a composite topping. The cross sectional Area of each of the girders with the topping is 425 in² with a moment of inertia of 78450 in⁴. The radius of gyration of each girder was

184.35 with a top section modulus of 3261.72 in³ and a bottom section modulus of 4140.23 in³. Figure 3.3 shows the cross section for each of the test specimens with the composite topping.



Figure 3.3 - Picture of specimen cross section

3.2.2 Steel Reinforcement and Strand Designation

Each of the test specimens shared the same cross section properties, but varied in the number and type of prestressing strands. All of the girders were prestressed with straight tendons except for test specimen number 6 which had six draped tendons. Each of the strands used were 7-wire bonded strands with a 7/16 inch diameter. There are a couple different patterns in the prestressing strand designation and non-prestressed steel placement. These different patterns would result in different ultimate moment capacities and deflections.

Girders 4, 5 and 8 shared the same steel pattern and strand designation. Each of these girders was originally constructed with two rows of eight 7/16 inch diameter prestressing strands and a row of four just above them. There were also two rows of 2 strands in the web of the girder and one row of 2 strands located in the top flange. Along with the prestressing strands, there were mild steel layers placed throughout the girders

near the ends of the girders. There was one row of 3 #4 mild steel rebar placed in the bottom flange, 2 rows of 2 #4 mild steel rebar placed in the web and 1 row of 2 #4 mild steel rebar placed in the top flange. The steel reinforcement designations for these girders can be seen in Figure 3.4.

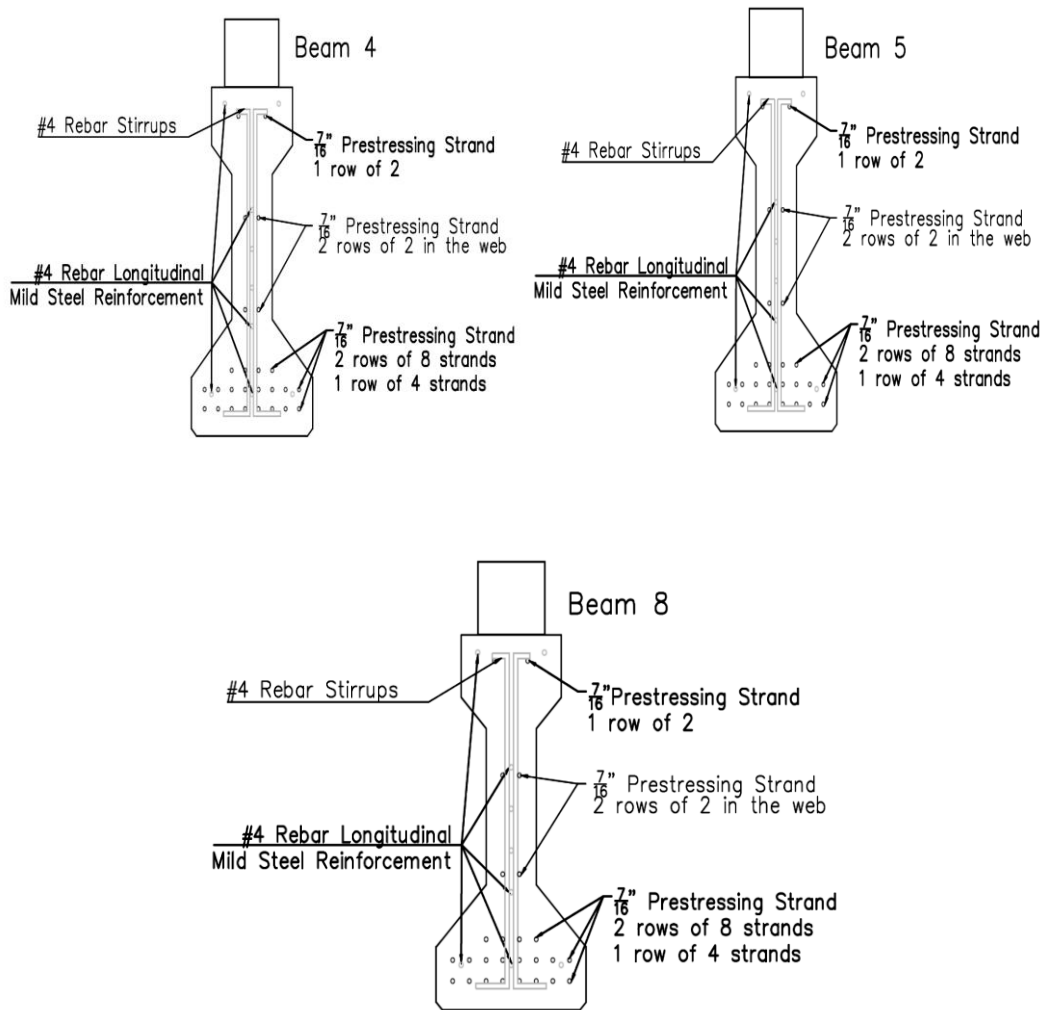


Figure 3.4 - Steel reinforcement patterns for girders 4, 5, and 8, provided by the Florida Department of Transportation (FDOT)

Girders 6 and 7 had different strand configurations than 4, 5 and 8. Girder 7 was originally constructed with 2 rows of 8 7/16 inch diameter prestressing strands in the bottom flange and 1 row of 4 in the top flange. Girder 7 had the same configuration of

mild steel as girders 4, 5 and 8. Girder 6 was originally constructed with 3 rows of 2 draped 7/16 inch diameter tendons through the web on the ends of the girder down to the bottom flange at midspan along with 2 rows of 6 and 1 row of four 7/16 inch diameter straight strands in the bottom flange. Girder 6 also has the same bar designation for the mild steel as all of the other girders. Figure 3.5 shows the cross-sections for girders 6 and 7.

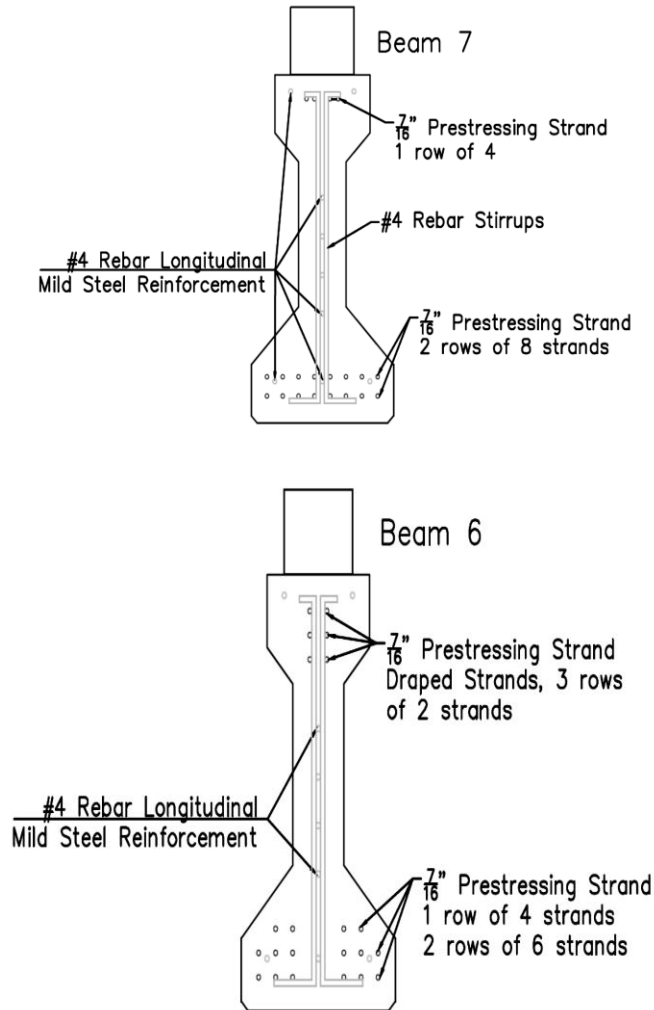


Figure 3.5 - Steel strand designation for girders 6 and 7 provided by the Florida Department of Transportation (FDOT)

Each of the test specimens was constructed with the same size stirrups and spacing for shear reinforcements. The girders were originally constructed with #4 sized

stirrups with 4 different spacing designations across the length. The first set was spaced at 4 inches apart for 12 inches as this section was closest to the supports where the shear forces are the largest. The next set of stirrups were spaced 6 inches apart for 18 inches followed by stirrups spaced at 1 foot apart for 8 ft. The final set was spaced at 16 inches to the centerline of the girder where shear forces are the least. The steel stirrups provided for each of the test girders was calculated to provide a shear capacity of 411 kips. The U-wraps were calculated to increase the shear capacity an additional 82.7 kips. For girder 6, which used the BASF carbon fiber material for the U-wraps, the shear capacity was calculated to increase by 48 kips. Figure 3.9 shows the spacing for the steel stirrups in each of the test girders.

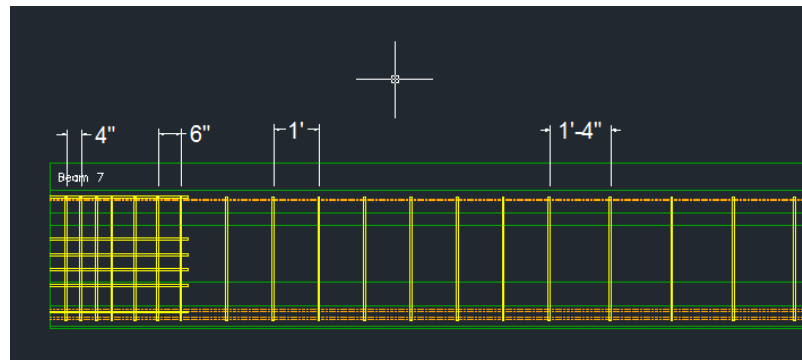


Figure 3.6 – Stirrup locations for shear reinforcement provided by the Florida Department of Transportation (FDOT)

3.2.3 Simulated Damage

With the exception of one of the control specimens, each of the rest of the test girders was subjected to simulated lateral damage. This damage was induced in the test specimens by making a saw cut at the mid-span of the girder through 3 of the prestressing strands which reduced the strength of the girders by 10.9% for girders 4 and 5, 12% for girder 7, and 8.9% for girder 6. Before the cut was repaired, the surface was roughened using chisels to help improve the bond surface. The cut was then repaired using mortar

and an epoxy injection to fill the cut and restore the bond of the concrete. Using a saw cut to simulate the damage also gave the advantage of having as close to a perfect repair of the concrete section as possible which would in turn result in the best performance of the CFRP. Figure 3.7 below shows a schematic for the simulated damage done to the test girders.

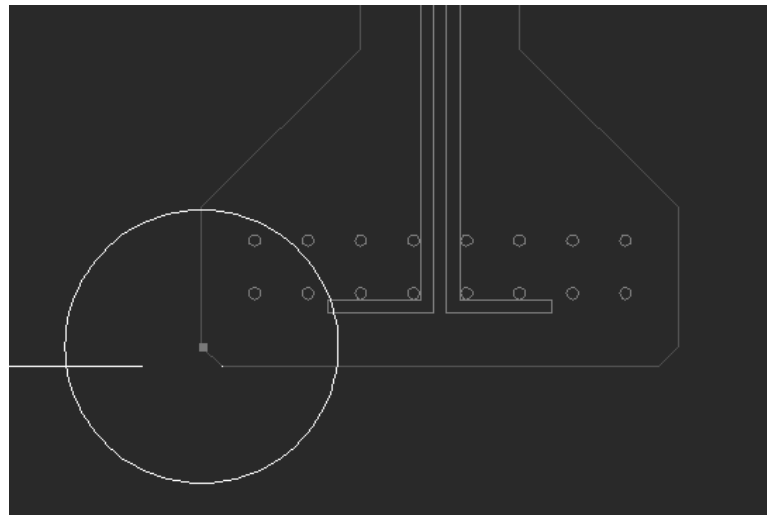


Figure 3.7 - Simulated damage area and strand schematic

3.3 Test Setup

Each of the test girders was tested in Tallahassee Florida at the FDOT structures lab. The five girders were tested under static loading conditions. All of the girders were tested in four-point bending with a hydraulic actuator mounted to a steel frame. Four-point bending allows for the girders to have a constant moment region between the two loading points and the shear spans from the support to the loading points which allows critical stresses to develop along a sizeable region instead of a single section (Larson et al, 2005). Four-point bending is also good for analyzing things such as debonding, CFRP

rupture and cracking in areas other than the mid-span where there is induced damage and failures are assumed to take place.

The load was applied by a hydraulic actuator positioned at the center of the girder that acts on a 100 inch long steel spreader beam. The load is transferred from the load cell and a round metal seating to the steel spreader beam which transfers the load to two points on the girder that are spaced 100 inches apart and centered about the mid-span. The spreader beam is supported on top of the test girder with rectangular rubber bearing pads.

The test girders are supported by rubber bearing pads placed on top of steel beams. The steel girders were placed in a rectangular shaped block made out of mortar which was on top of the floor of the lab. This rectangular block of mortar was made in order to spread the stresses caused by the loading of the machine across a larger area of the floor so that no damage was done to the floor of the lab. Figure 3.8 shows a picture of how the test girders were set up for testing in the FDOT structures lab in Tallahassee, FL.



Figure 3.8 – Picture of the testing setup in the FDOT structures lab

3.4 Instrumentation

There are a few different types of instruments used to analyze the test girders tested in a laboratory setting. These instruments include a load actuator, strain gauges and linear variable differential transformers (LVDT's). It is important that these devices are set up carefully and correctly so that they take accurate readings during the testing process. Each of the girders was tested with 15 strain gauges and 8 LVDT's while the load actuator was set up to push on a steel spreader beam that is 100 inches in length to separate the load so that 4-point bending is achieved.

3.4.1 Strain Gauges

Strain gauges were used to measure the different strains across the soffit of each girder as well as at different location throughout the depth of the girder as well. A total of 15 strain gauges were used for each girder with eleven of them place at different spacing's on the girders soffit and the rest at different levels of the centroid such as the center of gravity of the prestressing steel strands and the center of gravity of the girder and the top surface. Before the strain gauges were to be placed, the surface of the concrete had to be smoothed and flattened or the CFRP needed a flat smooth layer of adhesive applied before the two different surfaces were ready to have the strain gauges placed on them.

The first strain gauge placed on the soffit of the girder was placed at 52.75 inches away from the support. The next one was placed 56.5 inches from the first. Strain gauges 3 and 4 were equally spaced at 28.25 inches from strain gauge 2 toward the center of the girder. Strain gauge 5 was placed 27.75 inches from gauge 4 while gauge 6 was place at

midspan which was 34.5 inches from gauge 5. Gauge 11 was placed 11 inches from gauge 6 at midspan. Gauge 12 was then spaced 108.5 inches from gauge 11. Gauges 13, 14 and 15 were then spaced at 28.25, 27.75 and 28.25 inches.

There were four strain gauges placed throughout the depth of the girders at the midspan of the specimens. Gauge 7 was placed at 3.75 inches above the girder soffit at the centroid of the prestressing strands. Gauge 8 was placed at 23 inches above the soffit which is located on the web a few inches below the top flange. Gauges 9 and 10 were located on the top face of the girder at the midspan. Figure 3.9 displays the locations of the strain gauges throughout the depth of the girder as well as along the girder soffit.

3.4.2 Linear Variable Differential Transformers (LVDT's)

The deflections of the girder were measured using LVDT's which were placed in different sections of the girders to measure different deflections. There were a total of eight LVDT's for each girder with two on each end of the girder spaced 7.5 ft. from each other starting at the support. There were two LVDT's placed at the supports of the girder with the next two spaced at 7.5 feet from each end. Two more were placed at the support locations of the W24x176 steel loading girder which were another 7.5 feet towards the mid-span of the girder. Finally there were two placed on top of the girder at the centroid on both side of the girder to measure ultimate mid-span deflection as well as girder rotation due to loading and damaged strands. The locations of the LVDT's can also be seen from figure 3.9 as well.

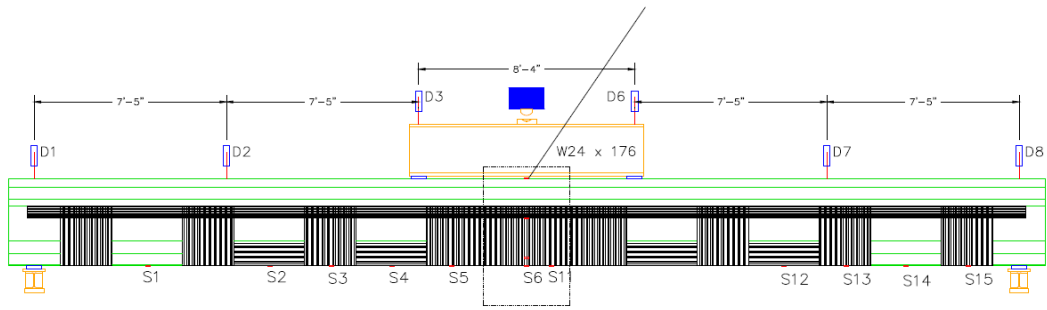


Figure 3.9 – Schematic for locations of strain gauges and LVDT's

3.5 Repair Configurations

Applying the proper configuration to repair the test girders can be the difference in a premature failure and a good repair. The configuration of the CFRP includes the number and length of the sheets applied to the girder soffit along with the number, length and width of the U-wrappings. The number of layers added to the girder soffit is the most important aspect of the configuration which adds the most strength to the girders ultimate flexural capacity. The U-wraps are generally used to anchor the layers on the soffit to help prevent debonding, but they also help in shear and resisting crack propagation. Some other measures taken to prevent crack propagation and debonding of U-wrappings were longitudinal strips placed on the sides of the bottom flange along with sheets placed on the sides of the web at mid-span underneath the U-wrappings in the longitudinal direction and a long strip underneath the top flange on top of the U-wraps.



Figure 3.10 – Finished repair of test girder in the lab

Each of the girders had been repaired with different configurations in order to find the effectiveness of each. There were two control specimens, girders 4 and 8, which were tested statically to failure for comparative measures. Girder 8 was undamaged without any CFRP added and girder 4 had simulated damaged done with only an epoxy injection and mortar repair, but no CFRP added. The other three girders were damaged and repaired with different CFRP configurations. Girder 6 used a combination of two different CFRP sheets because there was a shortage of the Fyfe brand material which made for a different spacing of U-wrappings because the width of the BASF material was less than that of the Fyfe material. Figure 3.11 illustrates the different U-wrap widths for the different products uses with the Fyfe material on the right side which is 24 inches and the BASF material on the left which was 20 inches in width.



Figure 3.11 – Example of different U-wrap widths for girder 6

Girders 5 and 7 were both damaged and repaired and had the same CFRP configuration except that there were a different number of layers on the soffit of each one. Girder 5 was designed with 2 layers of CFRP on the soffit while girder 7 had 3 layers. The U-wraps for both girders were spaced 32.5 inches apart with four of them placed side by side with a 1 inch overlap at the midspan. The width of each U-wrap was 24 inches and each girder was to have two layers of U-wraps at each of the locations. Each of the girders had longitudinal strips placed on the sides of the bottom flange for extra strength and to help prevent crack propagation. There was a sheet placed at midspan on both sides of the web underneath the U-wraps along in the longitudinal direction to also help prevent crack propagation. There was also a long strip placed just under the top flange on top of the U-wrappings to help prevent any unwanted debonding of the U-wrappings.

Girder 6 followed a similar configuration as girders 5 and 7 except that some of the U-wrappings were made from a CFRP manufactured by BASF which had some different properties than the Fyfe material. This girder was designed with two layers of

CFRP on the girder soffit which was made from the Fyfe material. The outermost U-wrappings were constructed from the Fyfe material while the rest were constructed from the BASF material which were only 21 inches wide so some adjustments needed to be made for symmetry. The configurations for each of the test specimens can be seen in figure 3.12 below.

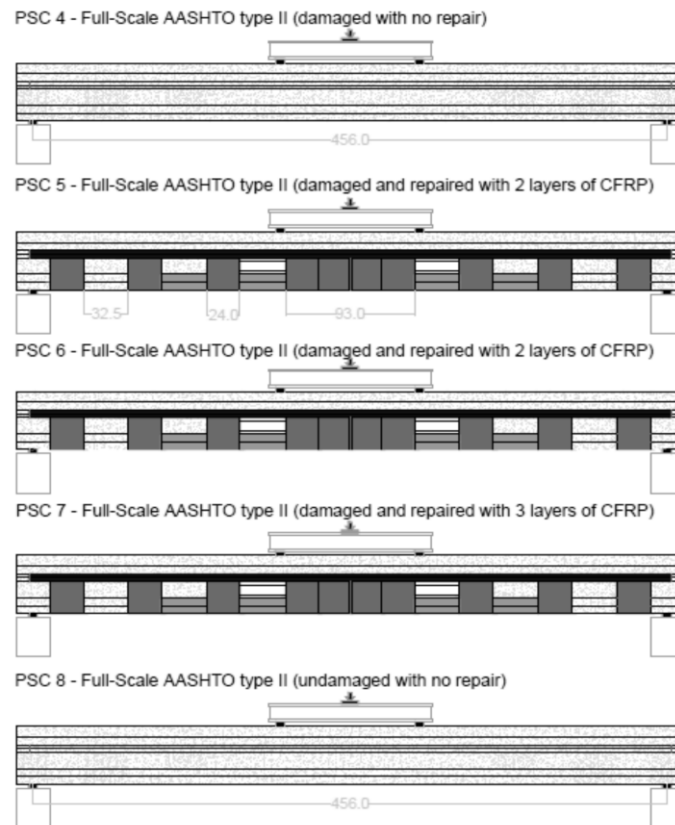


Figure 3.12 – Schematic for girder description and CFRP repair configurations

In the figure above, the widths for the U-wrappings other than the exterior U-wraps for girder 6 were different than the other repaired girders due to the different material used. The width of these inner U-wraps was 20 inches and spaced 36 inches apart.

Chapter 4

Results

This chapter presents the experimental data found from the damaged bridge girders repaired with CFRP sheets. Data to be considered are the loads, deflections and strain values which are taken from readings from software hooked up to the load actuator, strain gauges and LVDT's. The strain gauges were only capable of taking accurate readings up to 100 kips due to damage that occurred throughout the tests. Another important observation to be studied is the mode of failure for each of the girders. General observations were also examined such as cracking loads and patterns as well as loud noises during the testing. These observation parameters are then compared with analytical results from design criteria.

4.1 Control Girders

The control girders were used to have a reference against which to compare the repaired girder. One of the control girders, girder 4, had been damaged in the same manner as the other damaged girders except was not repaired in any way while the other control girder, girder 8, was undamaged and tested to failure. The simulated damage that was induced to control girder 4 was the same as the damage done to the repair girders which had shown to cause a 10.9% decrease in overall load carrying capacity. Table 4.1 shows a comparison of the max loading and maximum moment on the two control specimens.

	Moment-Capacity (kip-ft)	Maximum Load (kips)
Control Girder #4 (3 Strands Cut)	1237.05	166.83
Control Girder #8 (No Cut)	1373.4	185.22

Table 4.1 - Comparison of Control Girder Results

4.1.1 Control Girder 8

Girder 8 was the undamaged control girder which played a very important role. The ultimate strength of this girder provided the reference to which each of the repaired girders needed to reach in order to be considered successful repairs. The girder's ultimate moment was found to be 1373.44 k-ft. in the static flexural test. Figure 4.1 shows the load deformation plot for the experimental and analytical values of control girder 8. The strain gauges applied to the girder soffit and depth were recorded at intervals of 20 kips up to 100 kips before they became damaged and took bad readings. Figures 4.2 and 4.3 show plotted graphs for the strain distribution along the soffit of the girder and throughout the depth.

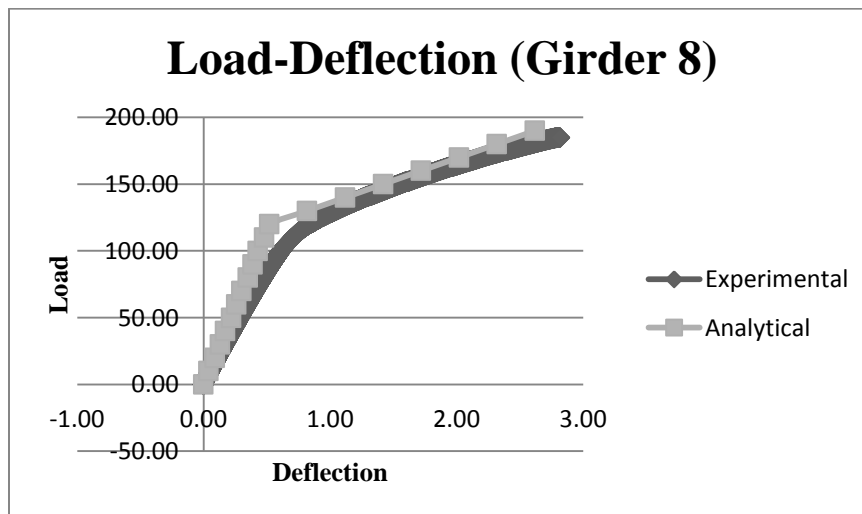


Figure 4.1– Load Deflection plot for girder 8

Figure 4.1 above shows the experimental load-deflection plot of girder 8 compared with the analytical model prediction. Girder 8 failed due to compression failure at mid-span in the top flange at a load of 185.22 kips and a deflection of 2.99 inches.

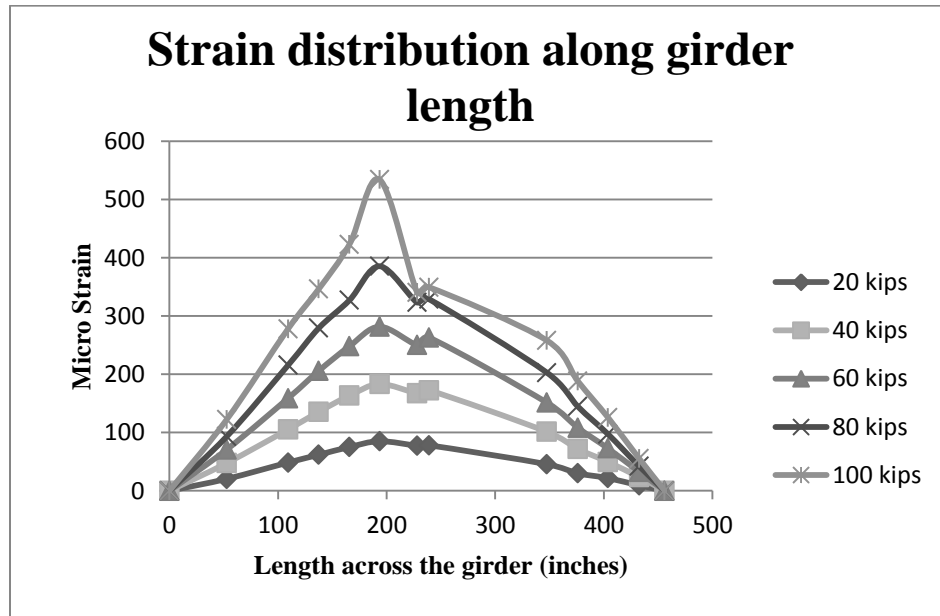


Figure 4.2 – Strain measured along the soffit of girder 8

The strain gauges along the soffit of control girder 8 recorded pretty good values until up around 100 kips. At this loading, you can see that there is very little change in strain from 80 kips to 100 kips at the strain gauge located at midspan which should show much more of an increase in tensile strain than was recorded, but had become damaged during the test.

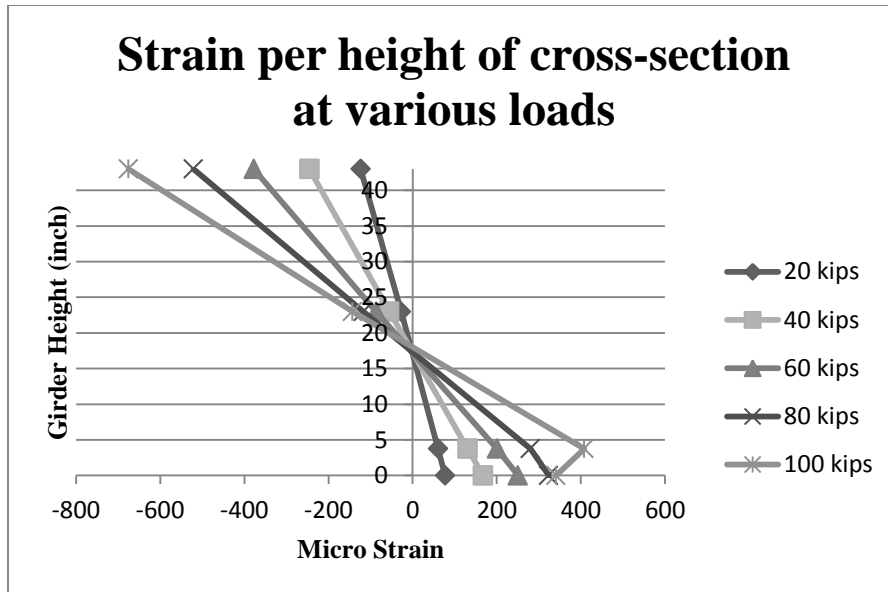


Figure 4.3 – Strain measured throughout the depth of girder 8

The strain gauges placed throughout the depth of girder 8 showed to be linearly distributed as the load increased up until about 80 kips where the strain gauge on the soffit had become damaged and stopped showing an increase in tensile strain. It can be seen on the graph where the strain in the gauge placed on the girder soffit stops increasing at about 80 kips.

4.1.2 Damaged Control Girder 4 (3 Strands Severed)

Control girder 4 had induced lateral damage done to it by saw cutting through 3 strands in the bottom flange as shown in chapter 3 from figure 3.7. This specimen was the girder that had the least amount of flexural strength for the experiment. The ultimate moment capacity of girder 4 was found to be 1237.04 k-ft. The girder experienced lots of large cracks propagating from the simulated damage point at midspan as well. The load-deflection plot for this girder is shown in figure 4.4. The plots for the two strain distributions can also be seen in figures 4.5 and 4.6.

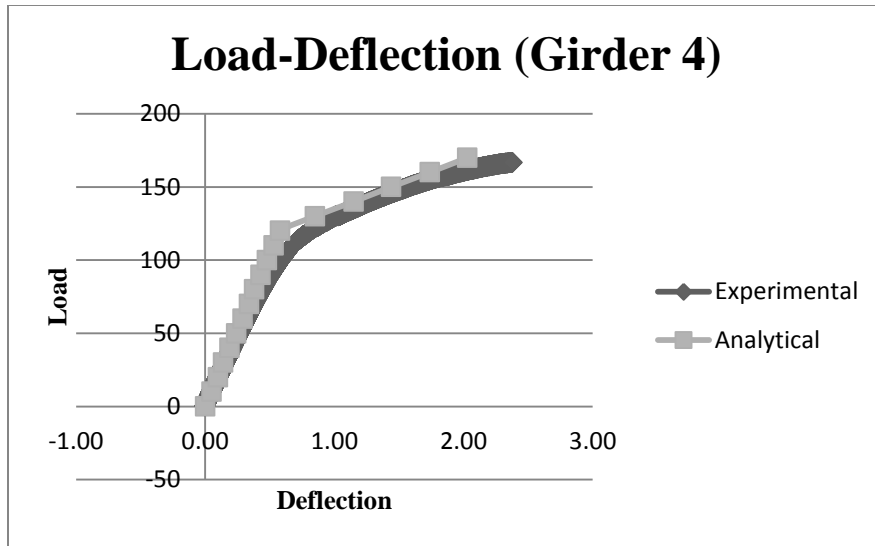


Figure 4.4 – Load deflection plot for girder 4

The deflection calculations of the damaged control girder had shown to be quite accurate using the bilinear method compared with the experimental results. Girder 4 had a compression failure at mid-span on the top fibers at a load of 166.8 kips and a deflection of 2.41 inches.

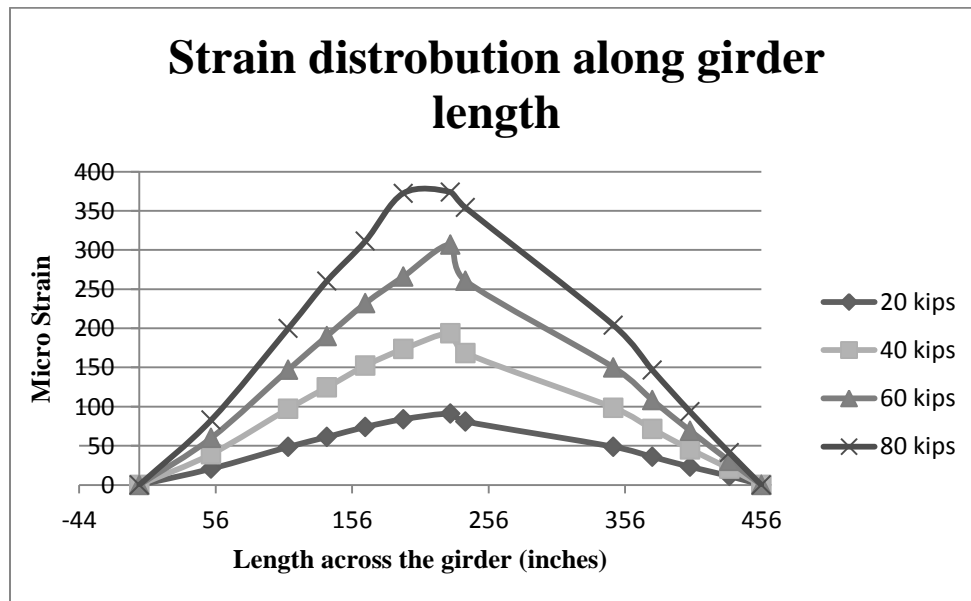


Figure 4.5 – Strain measured along the soffit of girder 4

The graph of the strain gauges attached to the soffit of girder 4 shows very good results compared to some of the other test girders. The results that were read by the strain gauges on each side of the girder seem to mirror each other and is expected to happen when a girder is subjected to flexural loading. Although the strain gauges show good results up to 100 kips, some of them still became damaged before the ultimate load was reached so the results at the failure load were not known.

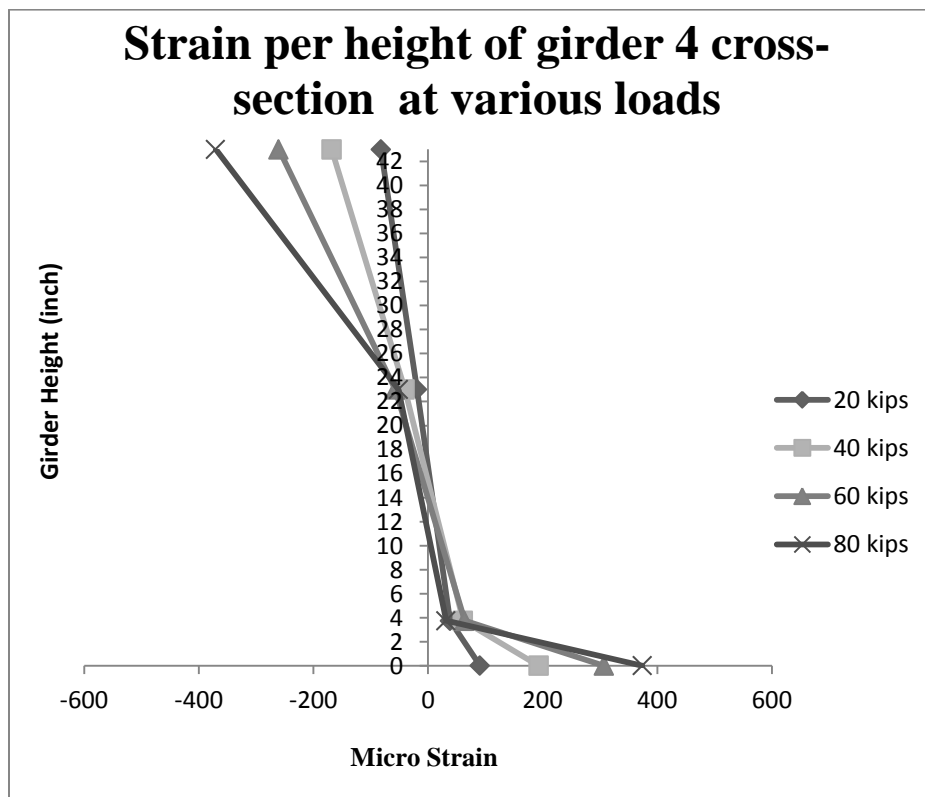


Figure 4.6 – Strain measurements throughout the height of girder 4

The strain gauges throughout the depth of girder 4 showed variable results. The strain gauge located at the center of gravity of the prestressing strands did not show much change throughout the loading while the gauge located on the soffit increased

significantly. It is believed that the strain gauge located at the center of the prestressing strands was not applied correctly.

4.2 Damaged and Repaired Girders

The following girders were damaged with a saw cut directly through 3 prestressing strands in the bottom flange then repaired with an epoxy injection and mortar before the CFRP was applied to the girders. These three girders had been repaired with different layers of CFRP to see which configuration would best work to bring each girder back to its original strength or higher. The results have shown that the repaired girders did better than just regain their capacity, but have also gained some extra strength as well.

4.2.1 Repaired Girder 5

Girder 5 was configured with 2 layers of CFRP along its soffit to repair the lost flexural strength from the simulated damage. There were small popping sounds between the concrete and the CFRP that started at about 110 kips and continued until the girder failed which was caused by cracking of the concrete. A small portion of the CFRP debonded from the bottom right hand side of the girder, but did not show to be very significant in the girder's failure. This girder showed to have a moment capacity of 1522.86 k-ft. Table 4.2 shows a comparison of the design and experimental results along with the percentage of increase in load that girder 5 reached compared to damaged control girder 8.

Girder 5	Moment-Capacity (kip-ft)	Maximum Load (kips)	% Change in capacity
Design flexural strength	1698.4	229.0	23.6% increase
Experimental Result	1522.86	205.4	10.88% increase

Table 4.2 - Calculated and experimental capacities of girder 5 compared to control girder 8

Figure 4.7 shows the experimental load deflection plot for girder 5 as well as the analytical load-deflection plot that was calculated in the spreadsheet. The strain

distribution graphs for the strain gauges attached along the soffit and the gauges attached throughout the depth of girder 5 can be seen in figures 4.8 and 4.9.

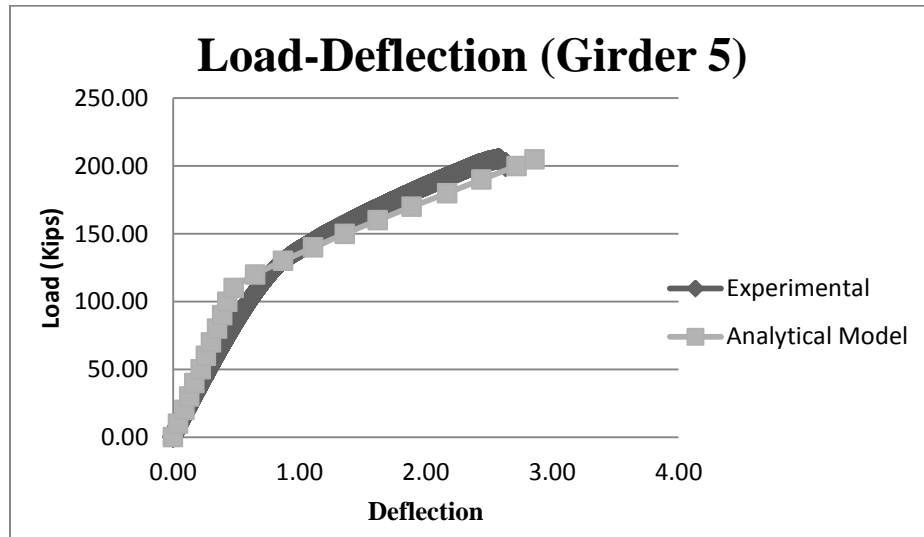


Figure 4.7 – Load deflection plot for girder 5

The load-deflection graph of girder 5 shown in the graph above also shows that the analytical model proved to be an accurate prediction of the girder's deflection. The girder experienced compression failure at a load of 205 kips with a deflection of 2.58 inches.

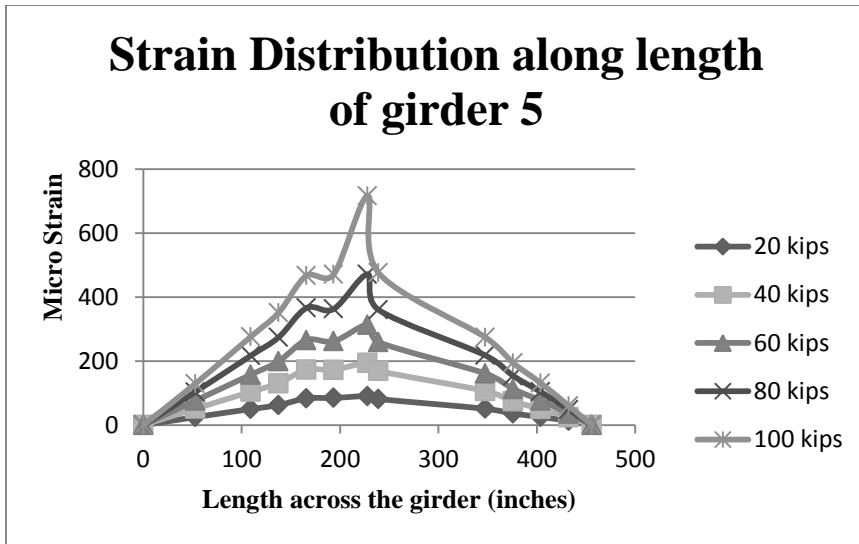


Figure 4.8 – Strain measurements distributed along the soffit of girder 5

The gauges that were placed on the soffit of girder 5 showed pretty good results compared to some of the other test girders before it became damaged. It can be seen that both sides of the graph seem to mimic each other which is the expected result of a flexural girder test. Although the strain in the soffit at the mid-span should be the greatest at this point, the sudden spike in the strain reading is unclear, but most likely due to cracking of the girder.

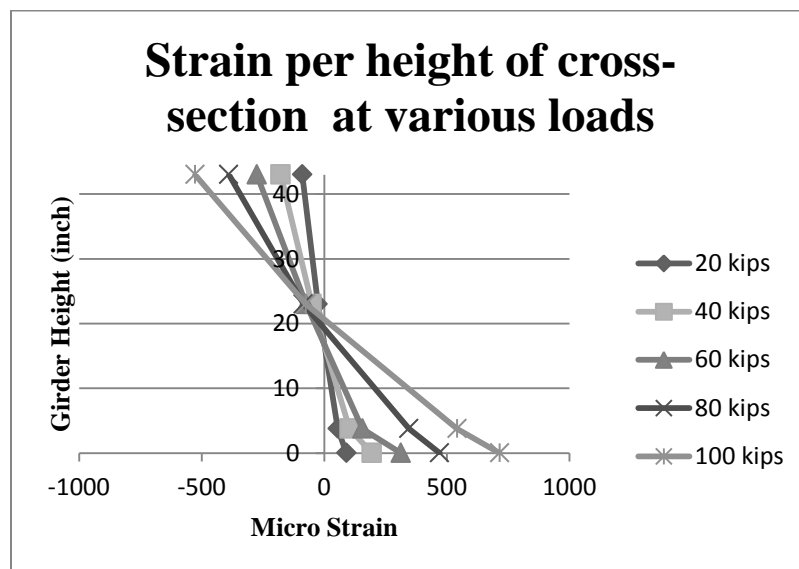


Figure 4.9 – Strain measurements throughout the height of girder 5

Girder 5 showed a pretty good strain distribution throughout its depth up until 100 kips before one of the strain gauges was damaged. It can be seen that the strains from the top to the bottom of the girder behave pretty linearly and evenly spaced with the loading increases which shows that they were taking good readings throughout the testing until they were damaged.

4.2.2 Repaired Girder 6

Girder 6 was also repaired with 2-layers of CFRP along the soffit of the girder. The end U-wrap anchorages of this girder were made of the same CFRP material as the soffit, but the U-wraps in between were constructed by a different product from BASF Chemical Company. Since the material properties of the BASF CFRP material were very similar to the Fyfe material, it was concluded that using this CFRP material as U-wrapping anchorages only, wouldn't affect the flexural capacity of the girder. The ultimate capacity of girder 6 was found to be 1592.5 k-ft. with a deflection of 4.94 inches. Visible cracks could be seen as early as 130 kips in the test. Table 4.3 shows the comparison between the design values and experimental results to those of control girder 8.

Girder 6	Moment-Capacity (kip-ft)	Maximum Load (kips)	% Change in capacity
Design flexural strength	1648.2	222.28	20% increase
Experimental Result	1592.5	214.77	15.9% increase

Table 4.3 - Calculated and experimental capacities of girder 6 compared to control girder 8

Figures 4.10, 4.11, and 4.12 show the load deflection plots the strain gauge readings along the soffit of the girder and the strain gauge readings throughout the depth of the girder.

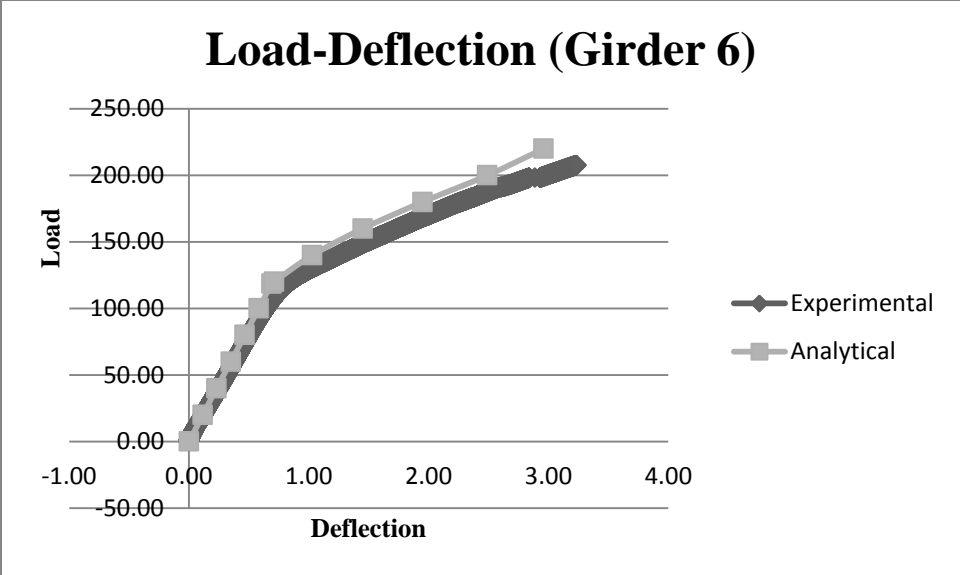


Figure 4.10 - Girder 6 load-deflection plot

The load deflection plot showed to be pretty accurate between the experimental and analytical values. Even with the different strand patterns and the use of draped strands, the deflection was calculated very accurately in the model.

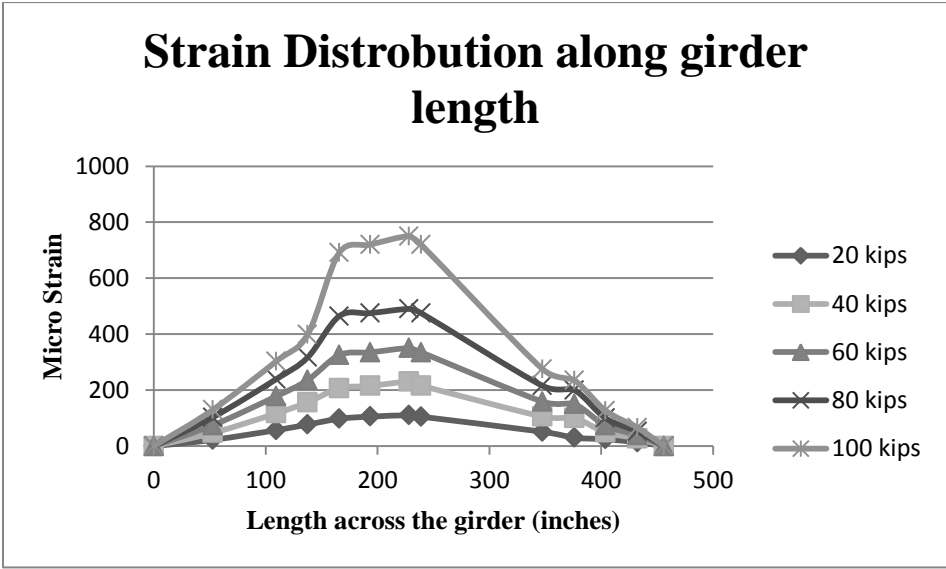


Figure 4.11 – Strain measured along the soffit of Girder 6

The strain measurements along the soffit of the girder other than strain gauge 6 located at midspan, gave pretty good readings up until around 100 kips. Gauge 6 was applied to an area where a large void had formed during the curing process of the epoxy which is believed to have caused the readings to be unusable. For the graph to show a realistic strain distribution, gauge 6 located at midspan of the soffit had to be left off.

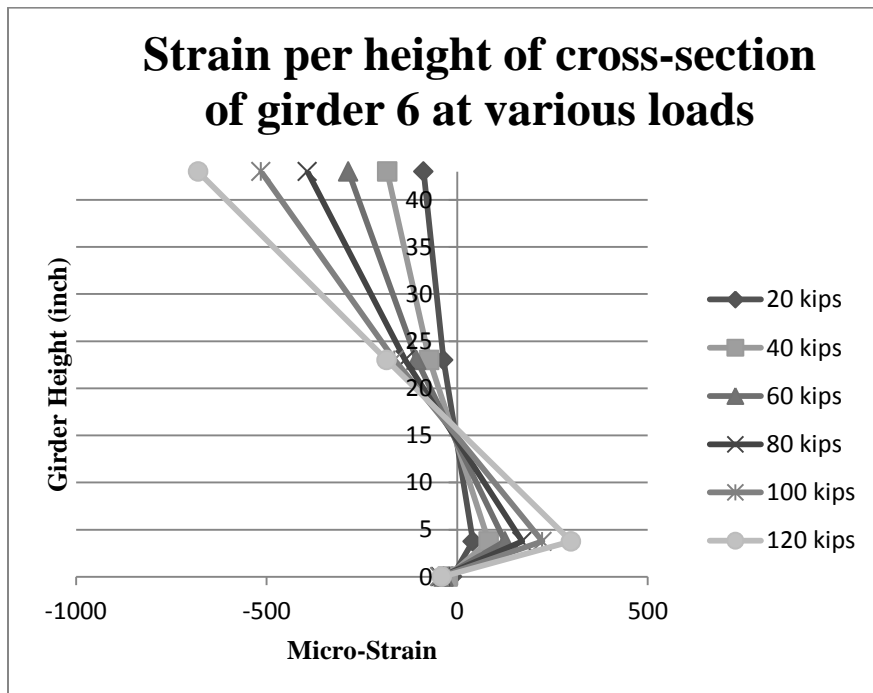


Figure 4.12 – Strain measurements throughout the height of girder 6

The strain gauge attached at the soffit at mid-span of girder 6 showed some unexpected and abnormal results. This strain gauge continued to show a decrease in strain until the load had surpassed the cracking load, then began to show increases in tensile strain. The result of this was most likely due to either a large void which developed in the soffit of the U-wrappings in the center of the girder while the epoxy cured or the strain gauge was placed incorrectly which might cause this abnormal behavior. This shows how

important that it is to make sure there are no voids and that the CFRP has a good bond with concrete and the longitudinal CFRP strips along the soffit of the girder as well as proper strain gauge placement. The rest of the gauges showed a pretty linear relationship from the change of compressive strain at the top of the girder down to the gauge located at the center of gravity of the prestressing strands.

4.2.3 Repaired Girder 7

To repair the loss of strength from the simulated lateral damage, girder 7 was configured with 3 layers of CFRP along the soffit of the girder. Although girder 7 was the only test girder with its prestressing strand configuration, it was designed with the same load carrying capacity as all of the other girders. It was also shown analytically in the model that the CFRP increased the girder capacity by 27.9%. Table 4.4 shows the comparisons between the design strength and the actual strength compared to the strength of control girder 8.

Girder 7	Moment-Capacity (kip-ft)	Maximum Load (kips)	% Change in capacity
Design flexural strength	1511.3	200	10.04% increase
Experimental Result	1529.8	205	11.38% increase

Table 4.4 - Calculated and experimental capacities of girder 7 compared to control girder 8

Figures 4.13, 4.14 and 4.15 show the load deflection plot, the strain distribution across the length of the girder and the strain distribution throughout the depth of the girder.

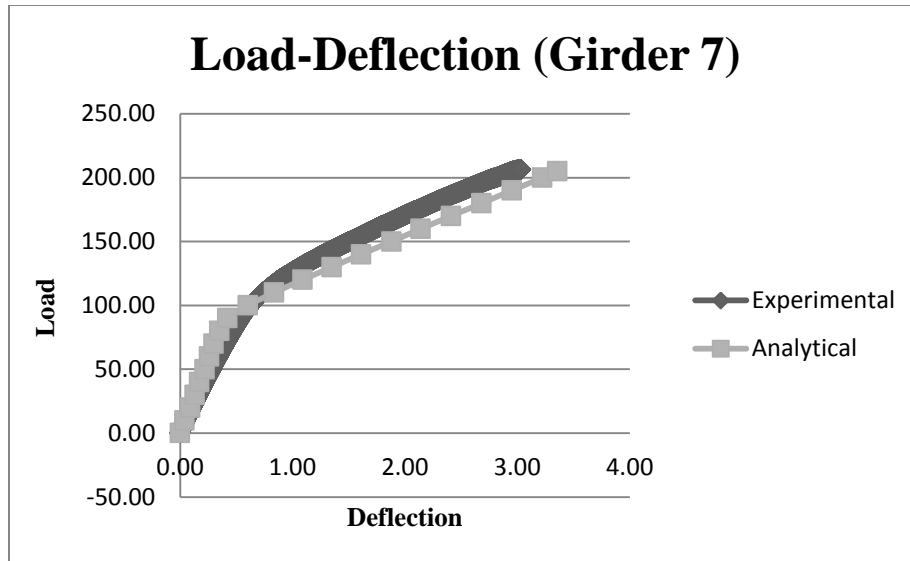


Figure 4.13 – Load deflection plots for girder 7

The load-deflection curve of girder 7 was in pretty close agreement with the curve done using the Microsoft excel spreadsheet. The girder failed due to a compression failure at a load of 206 kips and a deflection of 3.04 inches.

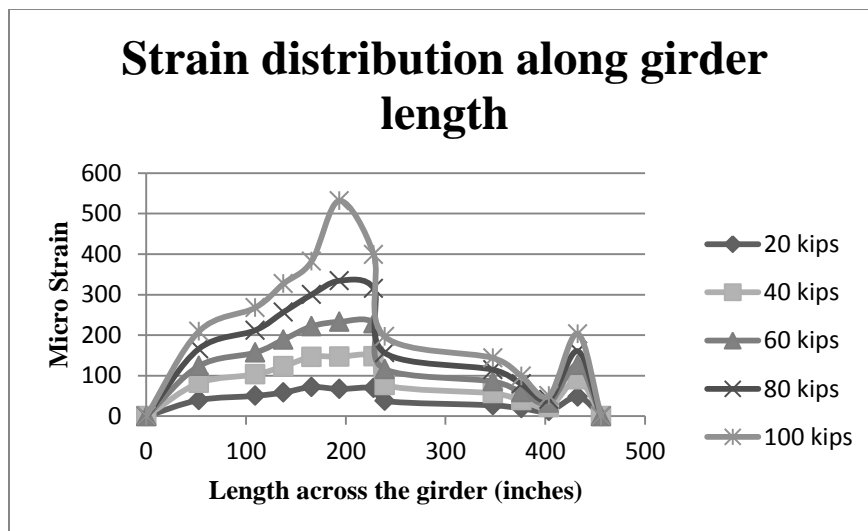


Figure 4.14 - Strain distribution along the length of the girder

From the strain distribution along the length of the girder you can see that the gauges which were placed on the far end of the girder were giving some odd results

compared to the ones on the other side. This could be the result of incorrect placement or premature damage, but it makes the analysis for those strain gauges tough to understand what is really happening at the CFRP level on that end of the girder. Strain gauge 15 was the only gauge on the far end that seemed to show similar results to gauge 1 which it is supposed to be close to in comparison.

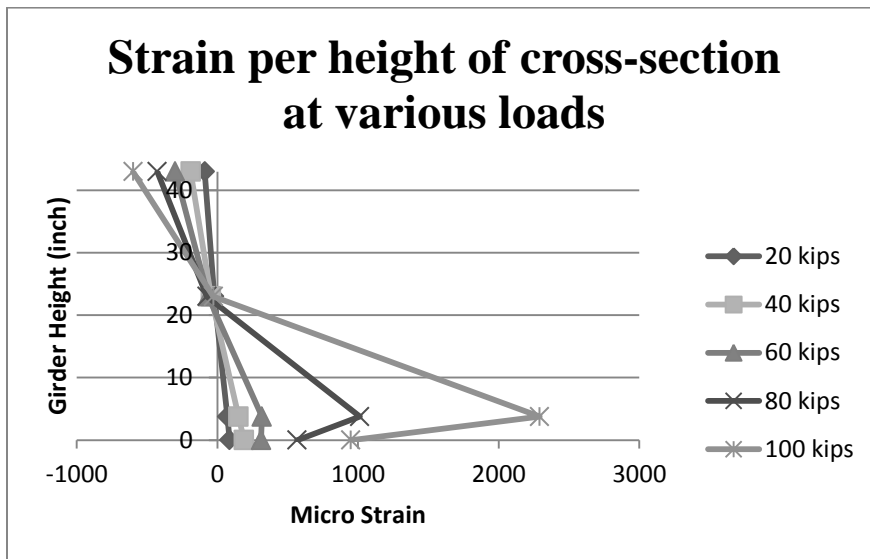


Figure 4.15 - Strain distribution throughout the depth of the girder

The strain gauges placed throughout the depth of girder 7 show a wide variation of differences in tensile strains. The tensile strains experienced at the center of gravity of the prestressing strands show much higher values as the load increases than that of the gauge values on the girder soffit.

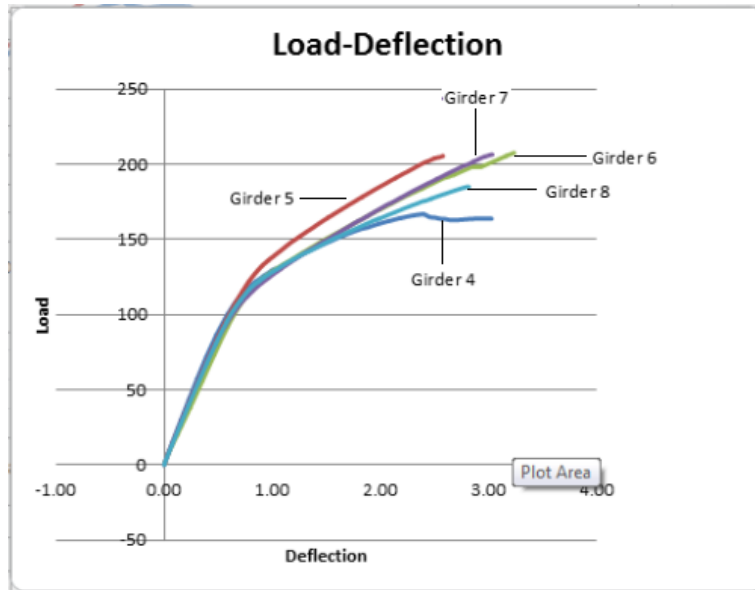


Figure 4.16 – Load deflection relationships of all tested girders

From the load deflection curve in figure 4.16, it can be seen that all of the repaired girders reached higher capacities than each of the control girders which shows that the repairs were successful. Before the cracking load was reached, each of the girders shows a similar linear pattern of deflection which changes for each of the girders after the cracking load was surpassed. Table 4.5 shows the results of the test girders in their moment capacity, deflection and failure mode.

Specimen	Moment Capacity (k-ft)	Deflection (in)	Failure Mode
4	1237.05	2.41	Concrete Crushing
5	1522.86	2.58	Concrete Crushing
6	1592.5	4.94	Concrete Crushing
7	1529.8	3.04	Concrete Crushing
8	1373.4	2.99	Concrete Crushing

Table 4.5 – Results of the test girders

Another factor that was observed throughout the experiment was the amount of rotation each girder experienced due to the 3 strands being cut on the one side of the bottom flange. To measure this, there were LVDT's placed on each side of the top of

each girder at mid-span and the difference between the two displacements gave the amount of rotation each girder experienced. The only test girder that experienced a significant amount of rotation was girder 6 which experienced a difference of 0.23 inches before it failed.

Chapter 5

Design and Analysis

5.1 Introduction

The analysis of the data was done using an excel spreadsheet that was developed over the course of the project. The spreadsheet was designed according to ACI 440.2R-08 specifications to determine the overall capacity of prestressed concrete bridge girders repaired with CFRP. The spreadsheet also calculates the deflections of reinforced and prestressed concrete bridge girders.

5.2 Pre-stress Loss Calculations

When prestressed concrete girders are cast, some of the initial prestressing force will be lost from a few different causes. Some of these losses occur quickly after the prestress transfer stage while some of the losses occur over long periods of time. Since the girders were cast in the 1960's, long term loss calculations needed to be made to determine the effective prestressing force in the strands. The calculations used to find the short and long term losses of the effective prestressing were done using methods presented in Nawy, 2002. The four losses that need to be accounted for when using pre-tensioned 7-wire bonded tendons are relaxation (RL), elastic shortening (ES), creep (CR) and the shrinkage (SH) losses.

Relaxation losses (RL) are a decrease in stress in the prestressing strands when the steel is subject to a constant strain. Elastic shortening losses (ES) are due to the shortening of the concrete when the prestressing force is applied which also causes the

same amount of shortening in the prestressing strands because they are bonded to the concrete. Creep losses (CR) are known as the deformation due to the longitudinal stresses from the prestressing force which occur over long periods of time. Shrinkage losses (SH) are due to the shrinkage of concrete due to many different factors such as humidity, curing time, size and type of aggregate, type of cement, mixture proportions and even the size and shape of the girder. These losses vary depending on four different factors such as the initial prestressing force, type of steel used, temperature and the age of the prestressed member.

The following calculations are used to determine the short and long term losses of prestressed girders from (Nawy, 2002).

Shrinkage Losses (SH):

$$SH = 8.2 \times 10^{-6} K_{SH} E_{PS} (1 - 0.06 \frac{V}{S}) (100 - RH) \quad 5.2.1$$

Where:

K_{SH} = Shrinkage coefficient

$\frac{V}{S}$ = Volume surface ratio

RH = Relative humidity

Creep Losses (CR):

$$CR = K_{CR} \frac{E_S}{E_C} (f_{cs} - f_{csd}) \quad 5.2.1$$

Where:

K_{CR} = Creep coefficient

(f_{cs}) = Net compressive stress in concrete at tendon Cgs right after prestress is applied

(f_{cds}) = Stress in concrete at tendon Cgs due to superimposed dead loads applied after the girder has been prestressed

Elastic Shortening Losses (ES):

$$ES = K_{es} E_s \frac{f_{cs}}{E_{ci}} \quad 5.2.3$$

Where:

K_{es} = Elastic shortening coefficient

E_{ci} = Modulus of elasticity of concrete at time prestressing is first applied

Relaxation Losses (RL):

$$RL = (K_{re} - J)(SH + CR + ES)C \quad 5.2.4$$

Where:

K_{re} , J , and C are coefficients found in tables

Total Losses (Δf_{pT}):

$$\Delta f_{pT} = CR + ES + RL + SH \quad 5.2.5$$

The calculated losses are added up and then subtracted from the initial prestressing force applied to get the effective prestressing force. It was calculated that the girders had a 22.5% loss in prestressing.

5.3 Capacity Calculations

The following calculations for the moment capacity were done according to the design recommendations in chapter 10 of the ACI 440.2R-08 document which calculates the ultimate load carrying capacity of a prestressed concrete girder with the application of CFRP. The ACI 440.2R-08 document does not give recommendations in regards to deflection calculations of strengthened concrete members.

Properties of the CFRP sheets are given by the manufacturer of the product to be used in the repair or strengthening of the specimen. These properties include the ultimate tensile strength of the CFRP (f_{fu}), the rupture strain (ϵ_{fu}), the modulus of elasticity of CFRP laminates (E_f), and the thickness per sheet (t_f). The geometric and reinforcement properties of the member to be repaired or strengthened should be known from the design specifications or should be calculated prior to the calculations with the CFRP application.

If an environmental reduction factor is to be used, the system design properties should be calculated by the following equations.

$$\begin{aligned} f_{fu} &= C_E f_{fu} & 5.3.1 \\ \epsilon_{fu} &= C_E \epsilon_{fu} \end{aligned}$$

Where C_E is the environmental reduction factor

The next step is to calculate the existing strains on the concrete girder soffit (ϵ_{bi}). There will be pre-existing strains in the concrete on the soffit at the time when the CFRP is placed so the strain in the CFRP will not be the same as the concrete strain which the fabric is bonded to. The strains in the concrete are due to different loads such as the dead weight of the girder, the prestressing load, and all other loads at the time of placement.

The following equation is used to determine the existing strain in the concrete soffit assuming the only loads on the girder at the time are prestressing loads and dead loads.

$$\epsilon_{bi} = \frac{-P_e}{E_c A_c} \left(1 + \frac{e y_b}{r^2}\right) + \frac{M_{DL} y_b}{E_c I_g} \quad 5.3.2$$

The design strain for the CFRP system is calculated next to determine the failure mode of the CFRP system. The failure modes include debonding of the CFRP from the concrete it is bonded to, and the rupture of the CFRP when it reaches its rupture strain. The maximum strain that the CFRP reinforcement can achieve is based on the failure mode in which the girder fails. These failure modes that the girder can undergo include concrete crushing (compression failure), CFRP rupture (tension failure), debonding of the CFRP reinforcement (tension failure), and prestressing steel rupture (tension failure). These limit states control the capacity for CFRP tensile strain. For a girder controlled by crushing of the compressive concrete, the effective design strain (ϵ_{fe}) in the CFRP can be calculated by:

$$\epsilon_{fe} = \epsilon_{cu} \left(\frac{d_f - c}{c}\right) - \epsilon_{bi} \leq \epsilon_{fd} \quad 5.3.3$$

This equation finds the effective strain level for any assumed depth of the neutral axis (c). The effective stress (f_{fe}) can then be calculated by multiplying this value by the modulus of elasticity of the CFRP reinforcement (E_f).

For a bridge girder in which the failure mode is governed by the rupture of the prestressing steel, the effective design strain in the CFRP reinforcement can be calculated from the following equation:

$$\epsilon_{fe} = (\epsilon_{pu} - \epsilon_{pi}) \left(\frac{d_f - c}{d_p - c}\right) - \epsilon_{bi} \leq \epsilon_{fd} \quad 5.3.4$$

Where ϵ_{pi} is the initial strain in the prestressing and is calculated by:

$$\epsilon_{pi} = \frac{P_e}{A_p E_p} + \frac{P_e}{A_c E_c} \left(1 + \frac{e^2}{r^2}\right) \quad 5.3.5$$

The debonding failure mode strain (ϵ_{fd}) can be calculated by:

$$\epsilon_{fd} = 0.083 \sqrt{\left(\frac{f'_c}{1 * E_f t_f}\right)} \quad 5.3.6$$

If the design strain is smaller than the rupture strain ($\epsilon_{fd} < \epsilon_{fu}$), then controlling failure mode of the CFRP is debonding, otherwise the failure mode of the system is CFRP rupture.

The ACI code includes a strength reduction factor (Φ) based on the ductility of the prestressing steel. “Adequate ductility is achieved if the strain in the prestressing steel at the nominal strength is at least 0.013 (ACI Committee 440, 2008).” The strength reduction factor would be reduced if the strain in the prestressing steel could not reach 0.013 because the failure would then be less ductile. The strength reduction factor for standard 270 and 250ksi strands can be calculated from the following conditional equations:

$$\Phi = 0.90 \text{ for } \epsilon_{ps} \geq 0.013 \quad 5.3.6$$

$$\Phi = 0.65 + \frac{0.25(\epsilon_{ps} - 0.010)}{0.013 - 0.010} \text{ for } 0.010 < \epsilon_{ps} < 0.013$$

$$\Phi = 0.65 \text{ for } \epsilon_{ps} \leq 0.010$$

Where ϵ_{ps} is the strain in the prestressing steel at nominal strength

At nominal strength, the strain level in the prestressing reinforcement (ϵ_{ps}) can be found through the following equation:

$$\epsilon_{ps} = \epsilon_{pe} + \frac{Pe}{A_c E_c} \left(1 + \frac{e^2}{r^2}\right) + \epsilon_{pnet} \leq 0.035 \quad 5.3.7$$

This equation is based on strain compatibility where (ϵ_{pe}) is the effective prestressing strain after losses are accounted for and (ϵ_{pnet}) is the net tensile strain in the prestressing reinforcement past the point of decompression at the nominal strength. The failure mode is the governing factor in the value of (ϵ_{pnet}). For the failure mode of concrete crushing, the following equation is used to find ϵ_{pnet} :

$$\epsilon_{pnet} = 0.003 \left(\frac{d_p - c}{c}\right) \quad 5.3.8$$

And for rupture or debonding of the CFRP reinforcement, the following equation is used:

$$\epsilon_{pnet} = (\epsilon_{fe} + \epsilon_{bi}) \left(\frac{d_p - c}{d_f - c}\right) \quad 5.3.9$$

The calculations to find the stress in the prestressing strands (f_{ps}) are dependent of the material properties of the prestressing steel. For the calculation of prestressing steel stress of 270 ksi 7-wire low relaxation strands, the following equation is used:

$$f_{ps} = 28,500\epsilon_{ps} \quad \text{for } \epsilon_{ps} \leq 0.0076 \quad 5.3.10$$

$$f_{ps} = 250 - \frac{0.04}{\epsilon_{ps} - 0.0064} \quad \text{for } \epsilon_{ps} > 0.0076$$

Internal force equilibrium must be checked for the stresses and strains calculated for the assumed depth of the neutral axis (c). The following equation is used to check if the assumed depth of the neutral axis is adequate for the internal force equilibrium:

$$c = \frac{A_p f_{ps} + A_f f_{fe}}{\alpha_1 f'_c \beta_1 b} \quad 5.3.11$$

In order for the internal force equilibrium to be satisfied, the above equation for the depth of the neutral axis must be equal to the assumed depth and if they are not equal, another assumption of the neutral axis must be made until the two values converge. The values of α_1 and β_1 are equivalent stress block factors whose values are dependent on the governing failure mode.

Once the convergence of the depth of the neutral axis is acquired, the nominal moment capacity (M_n) can then be calculated. There is an additional reduction factor (ψ_f) to be applied to the CFRP's flexural strength contribution. The ACI 440 code has given this reduction factor a value of 0.85. For calculating the nominal moment capacity, the following equation is used:

$$M_n = A_p f_{ps} (d_p - \frac{\beta_1 c}{2}) + \psi_f A_f f_{fe} (d_f - \frac{\beta_1 c}{2}) \quad 5.3.12$$

The calculations for the stress in the prestressing steel at service load conditions can be done based on the cracked and un-cracked condition of the section. The strain in the prestressing strands at service load can be calculated by the following equation:

$$\epsilon_{ps,s} = \epsilon_{pe} + \frac{P_e}{A_c E_c} (1 + \frac{e^2}{r^2}) + \epsilon_{pnet,s} \quad 5.3.13$$

This equation is the same as for the strain at nominal strength except that the $\epsilon_{pnet,s}$ value is the net tensile strain past the decompression zone in the prestressing strands at service load instead of at nominal load. The value of $\epsilon_{pnet,s}$ depends on the section properties of

the cracked or un-cracked member at service load. The following equations are used to find $\epsilon_{pnet,s}$:

For the un-cracked section at service load conditions:

$$\epsilon_{pnet,s} = \frac{M_s}{E_c I_g} \quad 5.3.14$$

For the cracked section at service load conditions:

$$\epsilon_{pnet,s} = \frac{M_{snet} e}{E_c I_{cr}} \quad 5.3.15$$

Where M_{snet} is the net service moment beyond the decompression zone

The stress in the prestressing steel can then be computed in the same manner as the stress for the strands at nominal strength.

The service load stresses in the CFRP is the final step in the design process. The initial strain on the girder soffit (ϵ_{bi}) depends on the section properties, cracked or un-cracked, at the time the CFRP is installed and at the service load conditions. “Prestressed sections can be uncracked at installation/uncracked at service, uncracked at installation/cracked at service, or cracked at installation/cracked at service (ACI Committee 440, 2008).” The Initial strain (ϵ_{bi}) will be calculated considering all loads on the member at the time of strengthening and the stress in the CFRP at the service load ($f_{f,s}$) can then be calculated using the following equation:

$$f_{f,s} = \left(\frac{E_f}{E_c}\right) \frac{M_s y_b}{I} - \epsilon_{bi} E_f \quad 5.3.16$$

The moment of inertia used in this equation is dependent on the condition of the section at service. If the section is uncracked, then the transformed gross moment of inertia (I_g)

will be used. If the section of the member is cracked, then the transformed cracked moment of inertia (I_{cr}) shall be used.

5.4 Shear Calculations

The shear capacity needed to be calculated to determine whether or not shear failures could be expected. When a concrete member is strengthened in flexure with CFRP, shear failure is also a concern because of the higher loads that the member can endure. First, the shear capacity from the concrete section and the steel stirrups needed to be calculated to figure out if the girders could hold the new loadings in shear as well as flexure or if additional strengthening needed to be applied through the use of traverse U-wraps or bonded CFRP face plates. The ACI 440 document gives some different shear strengthening techniques and specifications with CFRP.

The ACI 440 document gives the nominal shear capacity to be calculated from equation 5.4.1.

$$\Phi V_n = \Phi(V_c + V_s + \psi_f V_f) \quad 5.4.1$$

Where:

- V_c = Shear strength of the concrete section
- V_s = Shear capacity held by the steel stirrups
- V_f = Shear Capacity of the CFRP laminates

Equation 5.4.2 gives the shear strength of the concrete section found from the *ACI conservative method* when $f_{pe} > 0.4 * f_{pu}$

$$V_c = (0.60\sqrt{f'_c} + \frac{700V_u d_p}{M_u})b_w d_p \quad 5.4.2$$

Where:

- d_p = the larger value of the distance from extreme compression fiber to centroid of prestressing or $0.8 * h$
- V_u = Ultimate factored shear strength
- b_w = Width of the web

The shear capacity due to vertical stirrups can be calculated from equation 5.4.3 found in (Nawy, 2002).

$$V_s = \frac{A_v(f_y)d_p}{s} \quad 5.4.3$$

Where:

A_v = Area of shear reinforcement within a certain distance
 f_y = specified yield strength of shear reinforcement
 s = spacing between shear reinforcements

The shear capacity for the CFRP laminates is found from equation 5.4.4 defined in the ACI 440 document. Figure 5.4.1 shows the dimensional variables used in the calculations for shear strengthening.

$$V_f = \frac{A_{fv}f_{fe}(\sin\alpha + \cos\alpha)d_{fv}}{s_f} \quad 5.4.4$$

Where:

A_{fv} = Area of CFRP shear reinforcement calculated from equation 5.4.5 defined in ACI 440 document which is the product of the number, thickness and width of CFRP plies

$$A_{fv} = 2nt_fw_f \quad 5.4.5$$

f_{fe} = tensile stress in CFRP reinforcement. Calculated from equation 5.4.6 found in the ACI 440 document which is a product of the modulus of the fiber and the strain of the CFRP

$$f_{fe} = \varepsilon_{fe}E_f \quad 5.4.6$$

d_{fv} = Effective depth of shear reinforcement
 s_f = Spacing of CFRP shear reinforcement
 $(\sin \alpha + \cos \alpha)$ = The case of angled CFRP shear reinforcement

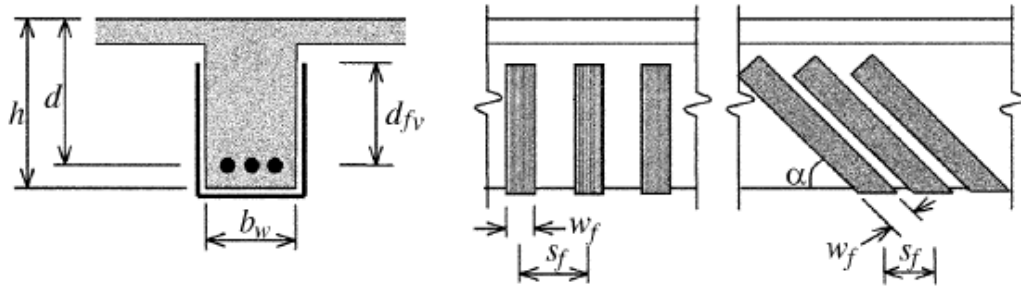


Figure 5.4.1 - Dimensional variables used in the calculations for shear strengthening courtesy of ACI Committee 440, 2008

5.5 Deflection Calculations

There are a few different ways to calculate predictions of the deflection of prestressed concrete girders strengthened with CFRP sheets, yet there are no guidelines or specifications defined. It was expected that girders strengthened with CFRP would have smaller deflections. The deflection calculations that were used to analyze the test girders followed both the effective moment of inertia method and the bilinear computation method. These two methods are slightly different, but will give good results.

5.5.1 Effective Moment of Inertia Method

The calculations for the effective moment of Inertia method to measure deflections will produce more of a curving line past the cracking moment on a plot compared to the bilinear method, which produces two linear plots on the graph due to the change in the moment of inertia after the cracking moment has been exceeded. The cracking moment is the moment that causes a tensile stress on the soffit of the girder greater than the concrete's modulus of rupture. The cracking moment due to live load only can be found by the following equation:

$$M_{cr} = S_b(7.5\sqrt{f'_c} + f_{ce} - f_d) \quad 5.5.1$$

Where:

S_b = Bottom section modulus of girder

$f_r = 7.5\sqrt{f'c}$ = Modulus of rupture

f_{ce} = Compressive stress at Cg due to the prestressing load only after the losses

f_d = Concrete extreme tensile stress due to unfactored dead load after cracking

While the cracking moment is larger than the applied moment, the effective moment of inertia will be equal to the gross moment of inertia. As the load surpasses the cracking moment and becomes larger, the effective moment of inertia will reduce from the value of the gross moment of inertia to the cracked moment of inertia. The effective moment of inertia can be found by equation 5.5.2 below.

$$I_e = \left(\frac{M_{cr}}{M_a}\right)^3 I_g + \left[1 - \left(\frac{M_{cr}}{M_a}\right)^3\right] I_{cr} \leq I_g \quad 5.5.2$$

Where:

M_{cr} = Cracking moment

M_a = Applied moment

I_g = Gross moment of inertia

I_{cr} = Transformed cracked moment of inertia

The effective Moment of Inertia can also be found by solving equation 5.5.3 for $\left(\frac{M_{cr}}{M_a}\right)$ and plug the value obtained into equation 5.5.2.

$$\frac{M_{cr}}{M_a} = 1 - \frac{f_{tl} - f_r}{f_L} \quad 5.5.3$$

Where:

f_{tl} = Final total stress

f_r = Modulus of rupture

f_L = Stress at extreme fibers due to live load

Once the effective moment of inertia has been found, calculating the deflection for the girder is easily done. The deflection calculations due to 3-point bending, 4-point bending and uniform loading conditions can be in figure 5.5.1. The gross moment of inertia is

used in each equation when the girder is uncracked while the effective moment of inertia (I_e) is substituted for the gross moment of inertia (I_g) in each equation when the girders are cracked.

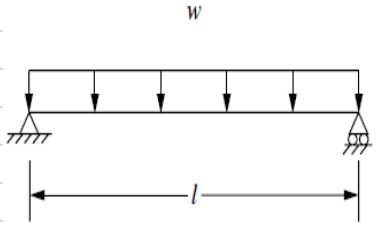
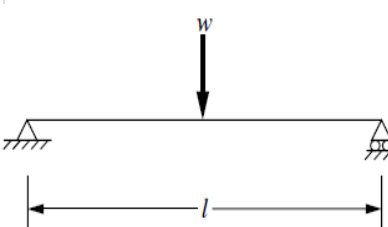
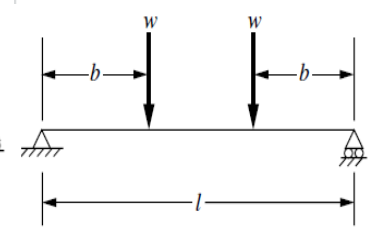
Uniform Load	3-Point Bending	4-Point Bending
 $\delta = \frac{5wl^4}{384EI} = \phi_c \frac{5l^2}{48}$	 $\delta = \frac{wl^3}{48EI} = \phi_c \frac{l^2}{12}$	 $\delta = \frac{wb}{24EI} (3l^2 - 4b^2)$

Figure 5.5.1 - Deflection equations for different loading conditions provided by Nawy, 2002

5.5.2 - Bilinear Method

The bilinear method calculates the deflection of the member in two stages which are the pre-cracking stage and the post cracking stage. “The ACI Code requires that computation of the deflection in the cracked zone in the bonded tendon girders be based on the transformed section (Nawy, 2002)”. The two linear plots for the gross moment of inertia and the cracked moment of inertia for the bilinear method moment-deflection curve can be seen in figure 5.5.2.

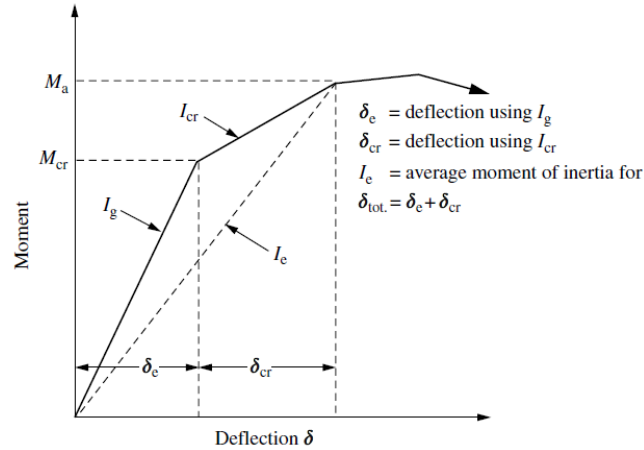


Figure 5.5.2 Bilinear moment-deflection relationship courtesy of Nawy 2002

The gross moment of inertia I_g and the cracked moment of inertia I_{cr} are the two main parameters when calculating the deflection using the bilinear method. Before the girders are cracked, the deflection calculations are quite simple and accurate. The gross moment of inertia is used in the calculations because the girder is still experiencing linear-elastic behavior. After the girders have been cracked, linear elasticity diminishes and the transformed cracked moment of inertia is used in the deflections. The gross moment of inertia is calculated from the geometry of the girder cross section, while the transformed cracked moment of inertia is found from equation 5.5.4.

$$I_{cr} = (n_p A_{ps} d_{ps}^2 + n_s A_s d_s^2 + n_f A_f d_f^2) (1 - 1.6 \sqrt{(n_p \rho_p + n_s \rho_s + n_f \rho_f)}) \quad 5.5.4$$

Where:

- n_p = Modular ratio of prestressing strands
- n_s = Modular ratio of mild steel
- n_f = Modular ratio of CFRP sheets
- A_{ps} = Area of prestressing steel
- A_s = Area of mild steel

A_f = Area of CFRP reinforcement
 d_{ps} = Depth to centroid of prestressing steel
 d_s = Depth to centroid of mild steel layers
 d_f = Depth of CFRP reinforcement
 ρ_{ps} = Reinforcement ratio of prestressing strands
 ρ_s = Reinforcement ratio of mild steel
 ρ_f = Reinforcement ratio of CFRP sheets

The cracking moment (M_{cr}) of the girders must also be calculated for the bilinear method as well as the effective moment of inertia method. Once the cracking moment been calculated, the cracking load can quickly be obtained which is when the transformed cracked moment of inertia needs to be used. The net stress on the bottom soffit of the girders needs to be found to figure out how much of the applied load is exceeding the modulus of rupture. The equation for this stress is calculated with the following equation.

$$f_{net} = (f_{cb} - f_r) \quad 5.5.5$$

Where:

f_{net} = Net stress on the girder soffit from live load
 f_{cb} = Total stress on the girder soffit due to all loads
 f_r = Modulus of rupture

When $f_{net} < 0$, the section has not been loaded enough for the girder to crack yet and the gross moment of inertia, I_g , can be used for the total deflection of the girder. If the net stress on the extreme fibers of the girder are >0 , then the girder is cracked so the cracked moment of Inertia must be used for the amount of loading beyond the girders cracking load. The next step is to find the tensile stress developed in the top fibers at the center of the girder due to the live load alone which can be found using equation 5.5.6 below.

$$f_t = \frac{(M_{LL}c_{gt})}{I_g} \quad 5.5.6$$

Where:

- M_{LL} = Moment due to live load
- C_{gt} = Center of gravity from the top of the girder
- I_g = Gross Moment of Inertia

Before the deflections can be calculated, the amount of load causing cracking in the girder must be calculated as well as the amount of load that exceeds cracking. The portion of load that does not cause cracking is found by using the following calculation:

$$w_{L1} = (f_L - f_{net})\left(\frac{w_L}{f_L}\right) \quad 5.5.7$$

Where:

- f_{net} = Total stress on girder soffit due to all loadings minus the rupture modulus
($f_{cb} - f_r$)
- w_L = Portion of live load that doesn't cause cracking
- f_L = Tensile stress developed in the top fibers of the girder due to the live load

The portion of load that exceeds the cracking load can be found by subtracting the portion of load that doesn't cause cracking from the total service load ($W_{service} - W_L$).

Once all of the above variables are calculated, the deflections can all be calculated.

The equations used to find the deflections for the bilinear method are the same as those for the effective moment of inertia method. Each method is the same for the pre-cracking stage as they both use the gross moment of inertia for the calculation. The difference between the two comes when the girder has cracked and the load is increasing. At this stage, the bilinear method uses the cracked moment of inertia (I_{cr}) in the calculations shown in figure 5.5.1 instead of the effective moment of inertia (I_e).

5.6 - Limitations

There are limitations for strengthened prestressed members under service load conditions to avoid undesirable failures in the prestressing strands, concrete and CFRP sheets (ACI Committee 440, 2008). The purpose of these limitations is so that the inelastic deformations in the prestressing strands and premature CFRP failures can be avoided. To prevent the prestressing steel from yielding, the stress in the steel should be less than or equal to 82% of the specified yield strength (f_{py}) at the service load levels or less than or equal to 74% of the specified tensile strength of the prestressing steel (f_{pu}). When fatigue is a concern, the compressive strength (f'_c) under service loading conditions of the concrete should also be limited to 45%.

Stress limits are also provided to avoid failures under sustained stresses as well as cyclic stresses. Creep-rupture is a phenomenon that happens when CFRP is subject to a sustained load over time which can cause the material to suddenly fail. The time period in which this occurs, called the endurance time, can decrease as the sustained tensile load increases along with exposure to adverse environmental conditions such as high temperature, ultraviolet light, high alkalinity, wet and dry cycles, or freeze-thaw cycles. Studies have shown that carbon fibers can sustain about 0.9 times their ultimate strengths before creep-rupture is encountered. Fatigue is caused from repeated cyclic loadings that can cause structural failure over time. The stress limit in the CFRP for sustained loading plus cyclic service loads is 0.55 times the design ultimate tensile strength of the fibers ($0.55f_{tu}$).

Limitations are also put on the overall amount of strengthening that a member can be strengthened with CFRP laminates. These limitations are set so that if the CFRP

material fails, the member can still support itself under a sustained service load. This is very important because there are many different reasons why the CFRP system could prematurely fail such as debonding.

Chapter 6

Conclusions and Recommendations

This chapter goes through the results of the experiment and draws conclusions and recommendations for future testing and uses for CFRP strengthening. Though the testing showed positive results, there are still areas that could be improved upon and mistakes that can be avoided in the future.

6.1 – Summary of Findings

The overall outcome of the experiment showed that strengthened girders could regain the capacity of the original girder and even achieve higher strengths. The predictions for the capacity using recommendations from the ACI 440-.2R document proved to be accurate. The deflection calculations based on the transformed cracked section bilinear analysis were pretty accurate as well.

Girder 5 experienced a 23.1% increase in strength compared to the damaged control specimen and a 10.8% increase compared to the undamaged control specimen. The girder experienced a small debonding issue on the right hand side of the soffit, but did not cause failure.

Test girder 6 also had its own prestressing strand configuration, but was designed with the same load carrying capacity as all the other girders. It also had a variation of different CFRP materials which had very similar properties so it was considered ok to use in the experiment. Girder 6 showed a 28% increase in strength than the damaged control

specimen and a 15.9% increase in strength from the undamaged control girder. Another observation made on this girder was the fact that it had rotated on its axis 0.23 inches in favor of the side that was damaged.

Test girder 7 showed good results, and like girder 6, it had the only strand configuration of its type, but was designed with the same load carrying capacity of all of the others. This girder showed an increase of 23.6% and 11.38% compared with girders 4 and 8, along with an increase of 27% that was shown analytically in the excel model.

6.2 – Conclusions

The conclusions of the experiment show overall positive results in the repair of the damaged girders. Observations made that could have affected the test results throughout the research project are listed below.

- The CFRP repair of damaged girders successfully restored their lost flexural capacity and increased it to be comparable to that of undamaged control girder.
- There was no premature debonding of the longitudinal CFRP sheets on the girder soffits. Although Girder 5 showed a small area that debonded near one of the loading points, it was not influential to the failure of the girder. This could be attributed to the U-wrapping configuration used.
- None of the test girders failed due to rupture of the CFRP. This shows that the CFRP material could have achieved higher strengths than observed in the experiment.
- There were no shear failures experienced by any of the test girders which could be attributed to an increase in strength provided by the U-wrappings.

- Minimum crack propagation at the damaged area was observed in any of the strengthened girders which may be the result of the longitudinal strips on the sides of the web and the bottom flange.
- There was no evidence of premature debonding of the U-wrappings which could be attributed to the strips placed on top of the U-wraps.

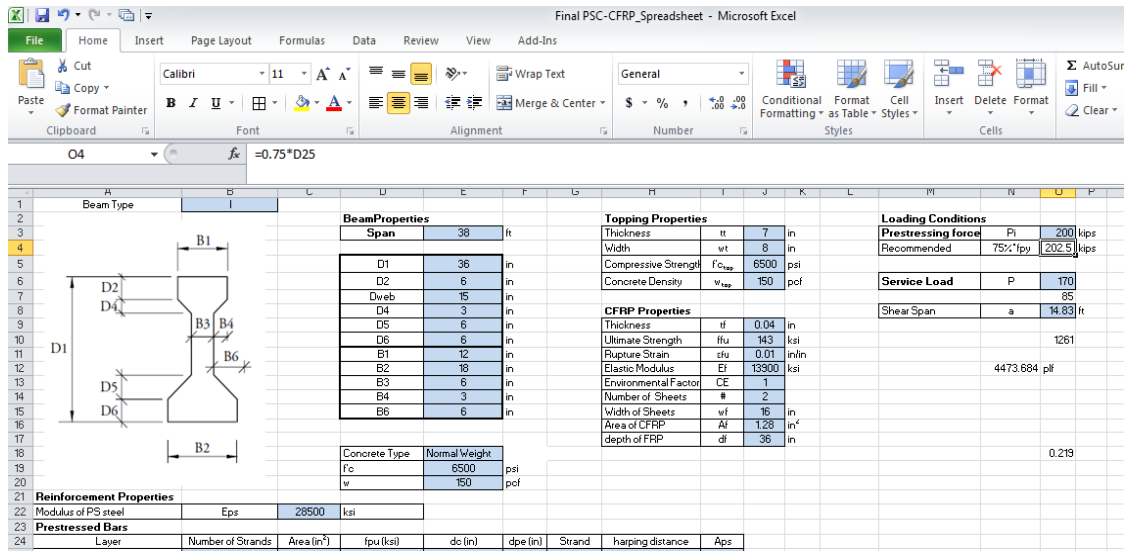
REFERENCES

1. ACI Committee 440, "ACI 440.2R-08 Guide for the Design and Construction of Externally Bonded FRP Systems for Strengthening Concrete Structures", *American Concrete Institute*, Farmington Hills, MI., 2008, pp. 80.
2. Kasan, J. L., "Structural Repair of Prestressed Concrete Bridge Girders", *MSCE Thesis*, University of Pittsburgh, Pennsylvania, 2009.
3. Nanni A., Huang, P.C. and Tumialan, J.G., "Strengthening of Impact-Damaged Bridge Girders Using FRP Laminates", *9th Int. Conf., Structural Faults and Repair*, London, UK., Engineering Technics Press, July, 2001.
4. Rosenboom, O. A., Miller, A. D., and Rizkalla, S., "Repair of Impact-Damaged Prestressed Concrete Bridge Girders using CFRP Materials", *ACSE Journal of Bridge Engineering*, accepted for publication 2011.
5. Grace, N. F., Ragheb, W. F. and Abdel-Sayed, G., "Flexural and Shear Strengthening of Concrete Girders Using New Triaxially Braided Ductile Fabric", *ACI Structural Journal*, V. 100. No. 6, November-December 2003.
6. Kasan, J.L. and Harries, K. A., "Repair of Impact-Damaged Prestressed Concrete Bridge Girders with Carbon Fiber Reinforced Polymers", *Asia-Pacific Conference on FRP in Structures*, Seoul, Korea, December 2009.
7. Reed, C.E., Peterman, R.J., Rasheed, H.A., "Evaluating FRP Repair Method for Cracked Prestressed Concrete Bridge Members Subject to Repeated Loadings Phase 1", *Kansas Department of Transportation*, Manhattan, Kansas, April 2005.
8. Shanafelt, G.O. and Horn, W.B., "Damage Evaluation and Repair Methods for Prestressed Concrete Bridge Members", *NCHRP Report 226*, Project No. 12-21, Transportation Research Board, Washington, D.C., 1980.
9. Rosenboom, O. A., and Rizkalla, S.H., "Fatigue Behavior of Prestressed Concrete Bridge Girders Strengthened with Various CFRP Systems", *North Carolina State University, 7th International Conference on Short & Medium Span Bridges*. 2006
10. Rosenboom, O.A., and Rizkalla, S.H., "Static behavior of 40 year-old prestressed concrete bridge girders strengthened with various FRP systems". *Proceedings of the Second International Conference on FRP Composites in Civil Engineering*, Adelaide, Australia, Dec. 2004.
11. Green, P. S., Boyd, A. J., and Lammert, K., "CFRP Repair of Impact-Damaged Bridge Girders, Volume I: Structural Evaluation of Impact Damaged Prestressed Concrete I Girders Repaired with FRP Materials", *BC-354 RPWO #55*, Florida Department of Transportation, 2004.

12. Tumialan, J.G., Huang, P.C, and Nanni, A., "Strengthening of an Impacted PC Girder on Bridge A10062", *Final Report RDT01-013/RI99-041*, Missouri Department of Transportation, 2001.
13. Carmichael, B.M., Barnes, R. W., "Repair of the uphapee creek bridge with frp laminates", Final Report RP-930-466-2, Alabama Department of Transportation, 2005.
14. Grace, N. F., Sayed, G. A., Soliman, A. K., Saleh, K. R., "Strengthening Reinforced Concrete Beams Using Fiber Reinforced Polymer (FRP) Laminates", *ACI Structural Journal*, Title no. 96-S95, September-October 1999.
15. Rosenboom, O.A., and Rizkalla, S.H., "analytical modeling of flexural debonding in CFRP strengthened reinforced or prestressed concrete beams", FRPRCS-8, *University of Patras, Patras, Greece*, July 16-18, 2007.
16. Fu, C.C., Burhouse, J.R. and Chang, G. L., "Study of Over-height Vehicles with Highway Bridges", Transportation Research Board, 2003.
17. Larson, K. H., Peterman, R.J., Rasheed, H. A., "Strength-Fatigue Behavior of Fiber Reinforced Polymer Strengthened Prestressed Concrete T-Beams", *Journal of Composites for Construction*. ASCE / July/August 2005
18. El-Tawil, S., Ogunc, C., Okeil, A., and Shahawy, M. (2001). "Static and Fatigue Analyses of RC Beams Strengthened with CFRP Laminates," *Journal of Composites for Construction*, November, 258-267.
19. Zobel, R.S. and Jirsa, J.O., "Performance of Strand Splice Repairs in Prestressed Concrete Bridges," *PCI Journal, Precast/Prestressed Concrete Institute*, Vol. 43, No. 5, November/December 1998, pp. 72-85
20. Akbarzadeh, H., and Maghsoudi, A. A., "Experimental and Analytical Investigation of Reinforced High Strength Concrete Continuous Beams Strengthened with Fiber Reinforced Polymer." *Materials and Design* (2009): 1130-147. Elsevier. Web. 10 Feb. 2012. <<http://www.elsevier.com/locate/matdes>>.
21. Hutchinson, R., Abdelrahman, A., and Rizkalla, S., "Shear Strengthening Using FRP Sheets for a Highway Bridge in Manitoba, Canada." Tech. Winnipeg: ISIS Canada Network of Centers of Excellence, University of Manitoba, 1997. Print
22. Razaqpur, A. G., and Isgor, O. B., "Proposed Shear Design Method for FRP-Reinforced Concrete Members without Stirrups." *ACI Structural Journal* 103.1 (2006): 93-102. Web. 3 Mar. 2012.
23. Buyukozturk, O., and Hearing, B., "Failure Behavior of Precracked Concrete Beams Retrofitted with FRP." Rep. N.p.: n.p., 1998. Print.
24. Feldman, Lisa R., James O. Jirsa, and Ramon L. Carrasquillo. Rep. no. 1370-1. Center for Transportation Research, The University of Texas at Austin, June 1996. Web. Mar. 2012. <<http://fsel.engr.utexas.edu/publications/docs/1307-1.pdf>>.
25. Harries, Kent A., Jarret Kasan, and John Aktas. "Repair methods for prestressed concrete girders." Tech. no. FHWA-PA-2009-008-PIT 006. Harrisburg, PA:

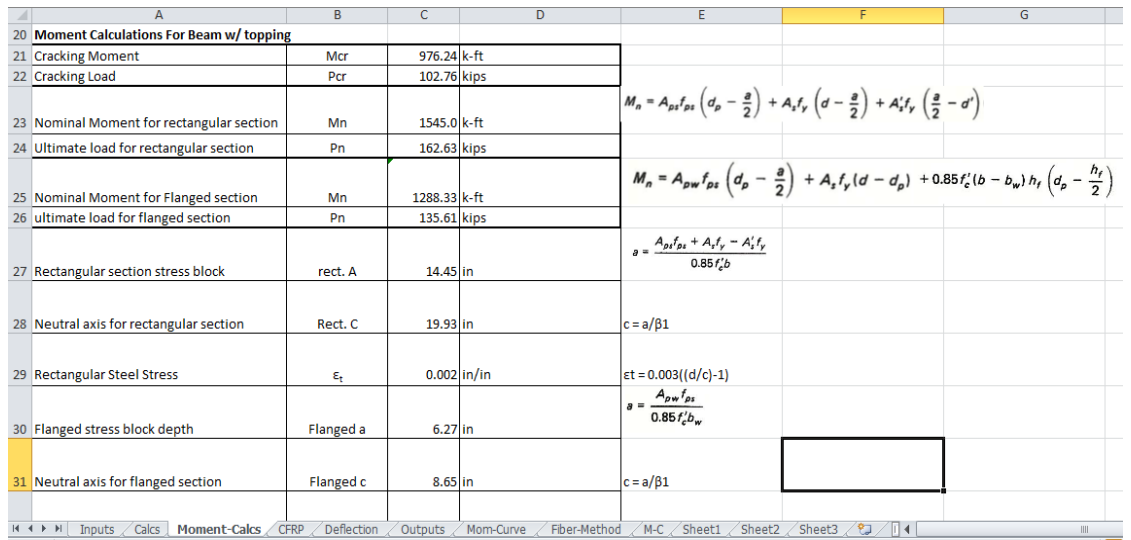
- Pennsylvania Department of Transportation, 2009. Web. Mar. 2012. <<http://ftp://ftp.dot.state.pa.us>>.
26. Wight, R., M. Green, and M. Erki. "Prestressed FRP Sheets for Poststrengthening Reinforced Concrete Beams." *Journal of Composites for Construction* 5.4 (2001): 214-220. Web. Mar. 2012. <<http://ascelibrary.org>>.
 27. Dai, J. G., Ueda, T., Sato, Y., and Ito, T., "Flexural strengthening of rc beams using externally bonded frp sheets through flexible adhesive bonding." Tech. Hokkaido: International Institute for FRP in Construction, 2005. Print.
 28. Lamanna, A. J., Bank, L. C., and Scott, D. W., "Flexural Strengthening of Reinforced Concrete Beams Using Fasteners and Fiber-Reinforced Polymer Strips." *ACI Structural Journal*, 2001. Print.
 29. Nawy, E. G. *Prestressed Concrete: A Fundamental Approach*. 4th ed. Upper Saddle River: Prentice Hall, 2002. Print.
 30. Nordin, Hakan, and Täljsten, B., "Concrete Beams Strengthened with Prestressed Near Surface Mounted CFRP." *Journal of Composites for Construction* 10.1 (2006): 60-68. *American Society of Civil Engineers*. Web. Apr. 2012. <<http://cedb.asce.org>>.
 31. Brena, S. F., Wood, S. L., and Kreger, M. E. *Using Carbon Fiber Composites to Increase the Flexural Capacity of Reinforced Concrete Bridges*. Rep. Austin, Texas: center for transportation research, the University of Texas at Austin, 2001. Web. Mar. 2012. <http://ftp.dot.state.tx.us/pub/txdot-info/rti/psr/1776_s.pdf>.
 32. Brena, S. F., Wood, S. L., and Kreger, M. E., "Full-Scale Tests of Bridge Components Strengthened Using Carbon Fiber-Reinforced Polymer Composites." *ACI Structural Journal* 100.6 (2003): 775-84. Web.
 33. Wipf, T. J., Klaiber, F. W., Rhodes, J. D., and Kempers, B. J., *Repair of Impact Damaged Prestressed Concrete Beams with CFRP*. Rep. Vol. 1. N.p.: Iowa Department of Transportation, 2004. Print
 34. Casadei, P., N. Galati, G. Boschetto, A. Nanni, K. Y. Tan, and G. Galecki. "Strengthening of Impacted Prestressed Concrete Bridge I-Girder Using Prestressed Near Surface Mounted C-FRP Bars." 2006. Web. April 12, 2012 from <<http://rb2c.mst.edu/media/research/rb2c/documents/C10.pdf>>.
 35. Vasiliev, V. V., and Morozov, E., "Advanced Mechanics of Composite Materials." (*Second Edition*). N.p., 2007. Web. 13 Dec. 2012.

Appendix A Spreadsheet Screen Shots



Inputs Tab

This tab of the model is where the user inputs the girder cross section, topping, prestressing/reinforcing steel and CFRP properties.



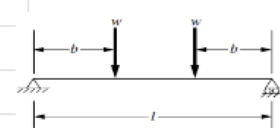
Moment Calculations

This tab which calculates the girder's moment capacity without the CFRP applied.

	A	B	C	D	E	F
42	Calculate Flexural Strength Components					
43	Prestressing steel contribution to bending (k-ft)	Mnp	1616.29	k-ft	$M_{Ap} = A_p f_{pu} \left(d_p - \frac{\beta_1 c}{2} \right)$	
44	FRP Contribution to bending (k-ft)	Mnf	193.92	k-ft		
45			1810.21	k-ft	$M_{Af} = A_s f_{fe} \left(d_f - \frac{\beta_1 c}{2} \right)$	
46	Calculate the design flexural strength of the section					
47	Strength Reduction factor	ϕ	0.9			
48	FRP Reduction Factor	ψ	0.85			
49	design Flexural Strength	ϕM_n	1603.0		$\phi M_n = \phi [M_{As} + \psi_f M_{Af}]$	
50						
51	Check Service Condition of the Section					
52	modulus of rupture (ksi)	fr	604.67	psi	$M_{cr} = \frac{f_r I_g}{y_b} + P_e \left(e + \frac{r^2}{y_b} \right)$	
53	Cracking Moment (k-ft)	Mcr	866.09	k-ft		
54						
55	Check Stress in prestressing steel at service condition					
56		$\epsilon_{ps,s}$	0.00524	in/in	$e_{ps,s} = e_{pe} + \frac{P_e}{A_c E_c} \left(1 + \frac{e^2}{r^2} \right) + \frac{M_s e}{E_c I_g}$	
57	Stress in Steel at service condition	fps,s	149.27	psi		
58						
59	Checks Servicestress limits					
60	Check 1	fps,s <= 0.82fpy	OK		$f_{ps,s} = \begin{cases} 28,500 e_{ps,s} & \text{for } e_{ps,s} \leq 0.0086 \\ 270 - \frac{0.04}{e_{ps,s} - 0.07} & \text{for } e_{ps,s} > 0.0086 \end{cases}$	
61	Check 2	fps,s <= 0.74fpu	OK			

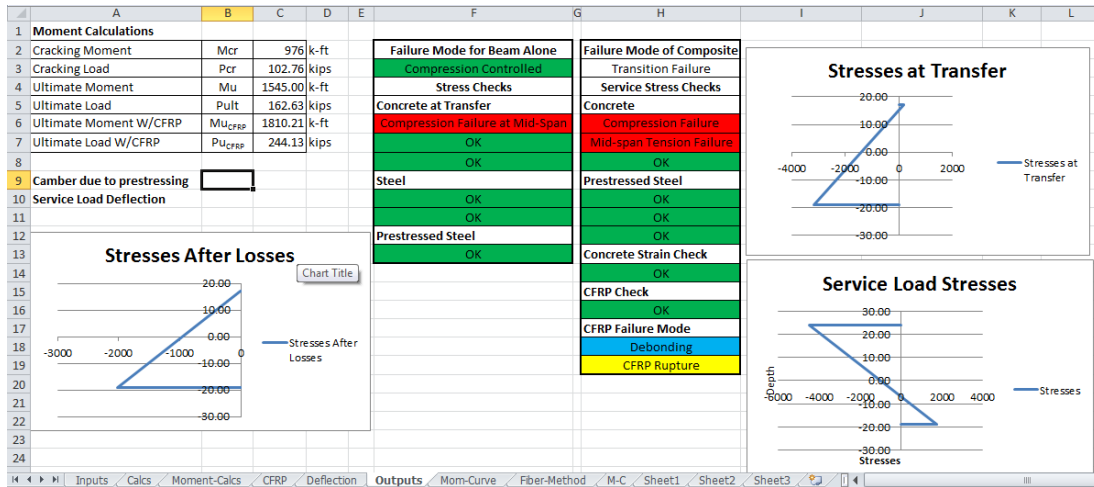
CFRP Calculations

This screen shot shows the moment calculations for the girders moment capacity with the CFRP applied.

1	Deflection Calculations				
2	Compressive stress at Cgc due to Pe	f _{ce}	-2224.84	psi	$f_{ce} = \frac{-P_e}{A_c} \left(1 + \frac{e_s c_s}{r^2} \right)$
3	Concrete stress at extreme fibers due to dead load	f _d	1114.07	psi	$f_d = \frac{W_d c_b}{I_g}$
4	Live Load Cracking Moment	M _{cr}	466.27	k-ft	$M_{cr} = S_b (7.5 \sqrt{f'_c} + f_{ce} - f_d)$
5	Gross Moment of Inertia	I _g	78450	in ⁴	$I_g = \sum (I_x + A d^2)$
6	Cracked Moment of Inertia	I _{cr}	18479	in ⁴	$I_{cr} = (n_p A_{ps} d_{ps}^2 + n_s A_s d_s^2 + n_f A_f d_f^2) (1 - 1.6 \sqrt{(n_p \rho_p + n_s \rho_s + n_f \rho_f)})$
7	Effective moment of Inertia	I _e	21515	in ⁴	$I_e = \left(\frac{M_{cr}}{M_a} \right)^3 I_g + \left[1 - \left(\frac{M_{cr}}{M_a} \right)^3 \right] I_{cr} < I_g$
8	Bottom Stresses due to Live Load	f _{bl}	3654	psi	$f_{bl} = \frac{M_s}{S_b}$
9	Net Stress in Beam Soffit	f _{net}	1056		$f_{net} = (f_{cb} - f_d)$
10	Portion of load not causing cracking	w ₁	120.88	kips	$w_{L1} = (f_L - f_{net}) \left(\frac{wL}{f_L} \right)$
11	Portion of load beyond cracking	w ₂	43.12		$w_2 = W_{service} - w_1$
12	Stress at bottom fibers	f _{cb}	1660	psi	
13	Applied Moment	M _a	1261	k-ft	
14	Deflection before Cracking	δ_g	0.817	in	
15	Deflection after cracking	δ_{cr}	1.002	in	
16	Total Deflection	δ_T	1.82		
17	Deflection Due to Camber	δ_{camber}	-0.165	in	

Deflection Calculations

This tab gives the calculations for all of the deflections due to prestressing forces as well as loading conditions with CFRP applied.



Outputs Tab

A sample of the outputs that the model gives the user aft